

1 **A selection of GMPEs for the United Kingdom**

2 **based on instrumental and macroseismic datasets**

3 Manuela Villani, Barbara Polidoro, Rory McCully, Ziggy Lubkowski, Thomas Ader, Ben
4 Edwards, Andreas Rietbrock, Tim J. Courtney and Martin Walsh

5 In countries with low-to-moderate seismicity the selection of appropriate ground
6 motion prediction equations (GMPEs) to be used in a probabilistic seismic hazard
7 analysis (PSHA) is a challenging step. Empirical observations of ground motion are
8 limited and GMPEs, when available, are generally based on stochastic simulations or
9 adjusted empirical GMPEs from elsewhere. This paper investigates the suitability of
10 recent GMPEs to the United Kingdom (UK). To this end, the spectral accelerations
11 obtained from available instrumental ground motion data in the UK, with magnitude
12 lower than 4.5 are compared with the GMPEs' predictions through the analysis of
13 residuals and the application of statistical tests. To compensate for the scarcity of data
14 for the magnitude range of interest in the PSHA, a macroseismic dataset is also
15 considered. Macroseismic intensities are converted to peak ground acceleration (PGA)
16 and statistically compared with the PGA predicted by the GMPEs. The GMPEs are
17 then compared in terms of median ground motion prediction through Sammon's maps
18 to evaluate their similarities. The analyses from both datasets led to six suitable
19 GMPEs, of which three are from the NGA West 2 project, one European, one is based
20 mainly on a Japanese dataset, and one is a stochastic GMPE developed specifically for
21 the UK. These GMPEs provide predictions that are consistent with the UK data and

22 can be used in the characterization of the ground motion attenuation in a PSHA in the
23 UK.

24 INTRODUCTION

25 The United Kingdom (UK) is a region of low to moderate seismicity for which a probabilistic
26 seismic hazard assessment (PSHA) is not always required. For ordinary constructions, seismic
27 hazard in the UK can be considered insignificant (Musson 2014). Booth et al. (2008) recommended
28 that that seismic actions should be explicitly considered for those structures where at least two out
29 of the three factors listed below apply:

- 30 1. Exceedance of regional seismic hazard at the site above a specified threshold. For the UK,
31 Booth et al. (2008) propose a threshold level based on the 2475 yr. return period peak
32 ground acceleration, PGA, on rock of at least 0.06 g.
- 33 2. The presence of soils overlaying rock at the site which might lead to a high amplification
34 of seismic actions.
- 35 3. The presence of unfavorable structural features.

36 Site specific PSHA in the UK is mandatory for strategic facilities such as nuclear power plants
37 (NPPs). The regulatory framework for nuclear facilities in the UK requires a formal and detailed
38 safety case to be submitted for NPP sites before permission to construct or operate can be granted.
39 As part of it, the seismic hazard should be estimated. Musson (2014) presented a history of seismic
40 hazard assessment for strategic facilities, highlighting that after a cessation of NPP construction in
41 Britain in 1995, in recent years steps have been taken towards a resumption of NPP building which
42 will see a need for new seismic hazard studies.

43 This study was developed as part of a seismic hazard assessment for a potential new nuclear site
44 in the UK, Wylfa Newydd in North Wales. However, the findings and the data presented in this
45 paper are not site specific and provide a suite of ground motion prediction equations (GMPEs) that
46 can be used for any generic site in the country.

47 The epistemic uncertainty related to the ground motion characterization (GMC) is due to the
48 uncertainty in the dynamic characteristics of the earthquake sources and of the wave propagation.
49 Generally, in a PSHA this epistemic uncertainty is handled through a logic tree approach (Kulkarni
50 et al., 1984). In a logic tree, each branch represents an alternative credible interpretation and all
51 the branches are assumed to be mutually exclusive and collectively exhaustive. The weights on the
52 branches represent the judgement about the credibility of the alternative models. These weights
53 are often called probabilities, but they are better treated as evaluations of the relative merits of the
54 alternative models (Abrahamson and Bommer, 2005). Scherbaum and Kuehn (2011) describe the
55 weights as subjective estimates of the degree of certainty or degree of belief that the corresponding
56 model is the one that should be used. In Musson (2012) they are described as the probability of
57 each model to be the “best model available”. In this context, same weight assigned to two different
58 models may reflect the fact that we don’t have a way to distinguish either of the models as superior
59 (Bommer, 2012).

60 Although multiple GMPEs are traditionally used in a logic tree to characterize the GMC, different
61 approaches have been used in recent seismic hazard assessments for NPPs to capture the epistemic
62 uncertainty in the ground motion characterization. There are numerous examples of the use of use
63 of a single or multiple GMPE as backbone and application of scaling factors to cover a broader
64 range of uncertainty (as for instance uncertainty in the stress drop parameters).

65 Examples of a scaled backbone approach can be encountered in the development of ground motion
66 models for PSHA applications in the Central and Eastern United States (CEUS), including Toro
67 et al. (1997) and Electric Power Research Institute (EPRI 2004, 2013a); Atkinson and Adams
68 (2013) used GMC logic trees for crustal earthquakes in active and stable regions, and also for
69 subduction earthquakes, in which the upper and lower branches carried models that are scaled
70 versions of a central “backbone” model. In the SSHAC (Senior Seismic Hazard Committee) Level
71 3 PSHA for the Thyspunt nuclear site in South Africa (Bommer et al., 2015), three GMPEs were
72 selected and, after the application of the host-to-target V_s - κ adjustments, they were scaled by four
73 scaling factors. In the Hanford project (Pacific Northwest National Laboratory, PNNL, 2014), a
74 backbone GMPE was developed from a small number of equations, and additional branches were
75 generated to capture the inherent epistemic uncertainty, including uncertainty in magnitude scaling
76 and host-to-target adjustments.

77 In regions such as the United Kingdom (UK), the epistemic uncertainty associated with ground
78 motion prediction is large and mainly due to the lack of strong motion data that can provide
79 knowledge on the nature of expected ground motions. This is especially true for the magnitude
80 range of primary interest for the seismic hazard (i.e. $M_w \geq 4.0$). Locally recorded ground motion
81 data only cover events up to 4.5 M_w , which corresponds to the Market Rasen earthquake of 2008
82 according to the magnitude estimation by Ottemöler and Sargeant (2010). Due to the lack of strong
83 motion data from the UK, there is a limited number of GMPEs derived specifically for the country.
84 Among these, the PML (1982, 1985 and 1988) models, derived in terms of surface wave magnitude
85 (M_s), have often been used for seismic hazard studies in the UK (e.g Arup, 1993; Goda et al.,
86 2013; Senior Hazard Working Party, SHWP, 2001). These models were not based on UK data, but
87 developed from a suite of selected records with similar magnitude and duration characteristics as

88 typical British earthquakes. These GMPEs are not considered in this study because they were
89 developed based on a limited datasets and the adopted regression methods are no longer considered
90 best practice. Bommer et al. (2011) highlighted that “the shortcomings of the PML (1988) spectral
91 prediction equations, when judged against the state-of-the-art in ground-motion prediction, are
92 many and serious”. Another UK specific GMPE was developed by Rietbrock et al. (2013) based
93 on stochastic simulations and on the work of Edwards et al. (2008). During the development of the
94 seismic hazard assessment for the Wylfa Newydd NPP, the original model of Rietbrock et al.
95 (2013) was updated and is therefore included in this analysis. This model is hereafter called
96 Rietbrock and Edwards (2017), RE17 and, since unpublished, is summarized in section
97 “SUMMARY OF THE RIETBROCK AND EDWARDS (2017) MODEL”. The methodology
98 upon which the GMPE is built is the same as in the original work of 2013, however new data were
99 implemented which led to a significant improvement in the ground motion predictions.

100 This study aims at evaluating the applicability of multiple GMPEs from worldwide and the
101 Rietbrock and Edwards (2017) model to the UK conditions. Given the scarcity of data in the UK
102 the use of multiple GMPEs is recommended since this allows to cover a wider range of spectral
103 shapes, as shown later in the paper. The following steps were adopted:

- 104 • Two ground motion datasets were compiled: one for the instrumentally recorded ground
105 motion which includes events with moment magnitude between 2.8 and 4.5 and one for
106 macroseismic observations for moment magnitude between 3.0 and 5.8;
- 107 • A pre-selection of the GMPEs was performed based mainly on the rejection criteria of
108 Cotton et al. (2006) and Bommer et al. (2010).
- 109 • The predictions from the GMPEs were compared with UK observations (instrumentally
110 recorded ground motion data and macroseismic intensities) in terms of residuals. The

111 statistical tests of Scherbaum et al. (2009) and Kale and Akkar (2013) are used to rank the
112 GMPEs and remove those that, although pass the rejection criteria, do not provide adequate
113 estimates of the ground motion; and

- 114 • The median predictions of the suite of GMPEs from above were compared using Sammon's
115 maps to evaluate similarities. The use of equations yielding similar ground motion
116 predictions in fact could lead to an underestimation of the epistemic uncertainty (Bommer
117 et al., 2015), undermining the benefits of using multiple GMPEs approach.

118 A suite of GMPEs is found to provide predictions that are consistent with the UK context and
119 can be adopted in a logic tree approach. According to the specific conditions of the site under
120 study, these GMPEs may then be adjusted through host-to-target adjustments and, if
121 appropriate, scaled to cover a wider range of epistemic uncertainty.

122 **SUMMARY OF THE RIETBROCK AND EDWARDS (2017) MODEL**

123 The original work of Edwards et al. (2008), upon which Rietbrock et al. (2013) was based, was
124 limited to single-component vertical short-period sensors. During the seismic hazard assessment
125 of the Wylfa Newydd NPP, the GMPE by Rietbrock et al. (2013) was updated. Two models were
126 developed: one for the UK and one site specific. In this paper, the model for the UK is summarized.

127 The upgraded digital broadband three component seismic network operated by the BGS since
128 2007 was adopted in the study. The data were processed in a consistent manner. Event location,
129 arrival times for the S- and P-waves, station locations and instrument calibration files were
130 provided by BGS. A signal to noise ratio analysis was performed to remove low quality signals.
131 187 signals were then processed (instrument corrected in velocity and band-pass filtered using an
132 acausal 6-pole Butterworth filter with corner frequencies set at the lowest and highest frequencies

133 at which the signal to noise ratio exceeded 3) and the 5% damped acceleration response spectra
134 were computed. As part of the study, the moment tensor solutions for recent UK events were
135 determined as well as the high frequency attenuation parameter κ_0 for many recording stations in
136 the UK using the approach of Anderson and Hough (1984) applied to larger magnitude UK events
137 ($M_L > 3.5$). Figure 1 shows the κ_0 values of the RE17 study as a function of V_{S30} as well as the
138 average values for each soil class: κ_0 was found to be approximately 0.03 s for soft soil
139 ($V_{S30} \leq 360\text{m/s}$), stiff soil ($360 < V_{S30} \leq 760\text{m/s}$) and rock ($760 < V_{S30} \leq 1,100\text{m/s}$), while a value of
140 0.012s was found at hard rock stations ($V_{S30} > 1,100\text{m/s}$).

141 Using the results of the spectral analysis, the seismological model used by Rietbrock et al.
142 (2013) for simulating strong ground-motion records in the UK was updated. In particular,

- 143 - Based on the average site amplification and H/V estimates determined during spectral
144 analysis, the GMPE is developed for a hard-rock model (V_{S30} of 2600m/s). The shear-wave
145 velocity profile for this model is based on the BGS's 1D UK model (Booth et al., 2001)
146 and a κ_0 of 0.005 s was adopted.
- 147 - The duration of shaking used for the model was also investigated. Due to the small
148 magnitude of recorded earthquakes, the measured duration is potentially affected by noise.
149 Direct measurement of the $D_{95=5\%-95\%}$ shaking duration using the new data and the
150 method proposed by Boore and Thompson (2014) led to increased durations with respect
151 to the model used by Rietbrock et al. (2013).

152 The seismological model was implemented in the simulation technique used by Rietbrock et
153 al. (2013) which uses the stochastic ground-motion method in the random vibration theory
154 framework (SMSIM, Boore, 2003), adjusted for moderate to large magnitude earthquakes for the

155 geometric effects related to the finite extent of rupture. Earthquakes of magnitude between 3 and
 156 7 and distances between 1 and 300km were simulated over a depth distribution consistent with UK
 157 seismicity.

158 Finally, the UK GMPE was derived following the same functional form as in Rietbrock et al.
 159 (2013) and reported below for ease of reference:

$$160 \quad \log_{10}(Y) = c_1 + c_2 M_W + c_3 M_W^2 + (c_4 + c_5 M_W) F_0 + (c_4 + c_5 M_W) F_0 + (c_4 + c_5 M_W) F_0 +$$

$$161 \quad c_{10} R \quad (1)$$

162 Where

$$163 \quad R = \sqrt{R_{JB}^2 + c_{11}^2} \quad (2)$$

$$164 \quad F_0 = \begin{cases} \log_{10}\left(\frac{10}{R}\right) & \text{for } R \leq 10\text{km} \\ 0 & \text{for } R > 10\text{km} \end{cases} \quad (3)$$

$$165 \quad F_1 = \begin{cases} \log_{10}(R) & \text{for } R \leq 50\text{km} \\ \log_{10}(50) & \text{for } R > 50\text{km} \end{cases} \quad (4)$$

$$166 \quad F_0 = \begin{cases} 0 & \text{for } R \leq 100 \text{ km} \\ \log_{10}\left(\frac{R}{100}\right) & \text{for } R > 100 \text{ km} \end{cases} \quad (5)$$

167 In the above equations Y is the ground motion parameter (peak ground velocity, PGV, peak
 168 ground acceleration PGA or spectral acceleration at selected periods, T , between 0.03 and 5 s), R_{JB}
 169 is the Joyner and Boore distance, and c_i are the regression coefficients provided in Table 1, along
 170 with the associated total, between-event and within-event uncertainties. Comparisons of the two
 171 models are shown in Figure 2 in terms of attenuation curves for three magnitude values ($M_w=4.5$,
 172 5.5 and 6.5) and two spectral periods ($T=0$ s, PGA, and $T=1$ s). The attenuation with distance
 173 follows a similar trend, however the new model leads to consistently higher predictions. Figure 2

174 shows the attenuation curves for PAG and spectral accelerations at T+1s for three magnitude
175 values ($M_w=4.5, 5.5$ and 6.5): the new model provides spectral acceleration that are larger than
176 Rietbrock et al. (2013) and, as we show later in the paper, are consistent with the UK ground
177 motion data.

178 **DESCRIPTION OF THE DATASETS ADOPTED FOR THE GMPES SELECTION**

179 To enable quantitative and qualitative comparisons with the GMPes predictions, we collated
180 UK ground motion data. The number of strong motion recordings in the UK is limited, particularly
181 for magnitudes greater than $M_w=4.0$ and therefore macroseismic intensity data were also included
182 to assist with the evaluation of GMPes. The two datasets are presented below. It is noted that these
183 two datasets were collated and analyzed independently of the ground motion data used to derive
184 the Rietbrock and Edwards (2017) model.

185 Data from nearby regions were excluded from this analysis. Sargeant and Ottomöller (2009)
186 determined the regional average Q_{Lg} and performed tomographic inversions in the frequency range
187 $1.0-10.0$ Hz to map the lateral variations in Q_{Lg} . They adopted a dataset of 64 earthquakes with
188 magnitude between 2.7 and 4.7 ML recorded at 93 stations. The spatial coverage of the data is such
189 that an estimate of regional average Q_{Lg} will be representative of most of onshore Britain. The
190 results of the study indicated that attenuation in Britain is slightly higher than in France and
191 significantly higher than in eastern North America and Scandinavia. A comparison of the Q_{Lg}
192 attenuation for various regions is provided in Figure 3. A decision was therefore made to limit the
193 dataset to UK events in order to avoid any bias due to differences in the attenuation characteristics.

194 UK INSTRUMENTAL DATASET

195 A dataset of instrumentally recorded ground motions was compiled for this study for
196 earthquake with moment magnitude greater than or equal to 3.0 and epicentral distances shorter
197 than 300 km. Overall, the dataset compiled for this study consists of 83 accelerograms (two
198 horizontal and one vertical component) from 12 earthquakes recorded in the UK from 1996 to
199 2018 with moment magnitude between 3.2 and 4.5. A summary of these earthquakes is presented
200 in Table 2. The location of these events and recording stations is shown in Figure 4 while Figure
201 5 shows their distribution in terms of magnitude versus (a) distance, (b) soil conditions and (c)
202 peak ground acceleration (PGA). Four moderate size events in the UK have been recorded by the
203 British Geological Survey, BGS, network since 2002. These are the 2002 Dudley earthquake with
204 $M_w=4.2$ (Sargeant and Ottömöller, 2009, consistent with Baptie et al., 2005, who found previously
205 $M_w=4.1$), the 2007 Folkestone earthquake with $M_w=4.0$ (Ottömoller et al., 2009; Ottömoller and
206 Seargeant, 2010), the 2008 Market Rasen earthquake with $M_w=4.5$ (Ottömoller and Seargeant,
207 2010) and the 2018 Swansea earthquake with local magnitude according to the BGS website
208 $M_L=4.6$ (converted to $M_w=4.3$ using the empirical correlation by Grünthal et al., 2009). The
209 information (metadata) on the causative earthquakes, source to site distance metrics and local site
210 conditions at the recording stations was compiled. The source parameters of the events were taken
211 from Ottemöller and Sargeant (2010), Sargeant et al. (2008), Baptie et al. (2005) and Sargeant and
212 Ottemöller (2009) for all the events up to 2008. The parameters for the 2014 Bristol Channel and
213 2015 Ramsgate events were calculated specifically for this study (Rietbrock and Edwards, 2017).
214 The parameters for the Llyn peninsula and Swansea earthquakes are those provided on the BGS
215 website and converted to moment magnitude as mentioned above.

216

217 Time history records were provided by the BGS who already performed the instrumental
218 correction and the signal to noise evaluation. The records were then processed through a baseline
219 correction and band-pass filtered using an acausal 4-pole Butterworth filter with corner frequencies
220 at 0.01 and 50Hz and the 5% damped acceleration response spectra were computed. A visual check
221 on the quality of the data and the associated response spectra was performed. It is highlighted that
222 among all the data, one record from the Folkestone earthquake led to the maximum PGA recorded
223 in the UK (PGA=0.1g) corresponding to the TFO station. However, the time history appears to be
224 saturated. After discussion with BGS, the record was kept in the dataset with consideration that a
225 maximum PGA of at least 0.1g is associated to that earthquake.

226 An understanding of site conditions at the stations locations is required to compare GMPEs
227 predictions against the observed ground motion recordings. Since in-situ measurements of shear
228 wave velocity (V_s) are not available for the majority of stations, the site conditions (Table 3) were
229 estimated based on a joint evaluation of the following information:

- 230 - Geological descriptions from the BGS. The ranges of V_{s30} (the average shear wave velocity
231 of the upper 30 m) associated with the description of geology are based on Borchedt (1994)
232 for all stations except for the PGB1 station, which is based on Christensen et al. (1980);
- 233 - Horizontal-to-vertical (H/V) Fourier Amplitude spectral ratios from recorded ground
234 motions computed in this study (Rietbrock and Edwards, 2017). Although based on
235 response spectral ratios, the site class classification proposed by Di Alessandro et al. (2012)
236 who considered earthquakes with M_w between 4.0 and 6.8 within 50 km of a seismometer
237 was used as a guide. When not consistent with the known geological information, the latter
238 was relied upon to assign a V_{s30} value; and

239 - Tallet-Williams and Fenton (2015) who carried out non-intrusive testing of three BGS
240 stations. Only tests at two of them yielded V_{S30} values; these are CCA1 and SWN1 with
241 values of 845 and 503 m/s respectively.

242 Table 3 presents a summary of the above information and the preferred V_{S30} value assigned to
243 each station for this study.

244 UK MACROSEISMIC DATA

245 The macroseismic dataset for this study comprises an extract of the UK Historical Earthquake
246 Database from the BGS website. All earthquakes with a magnitude greater than or equal to
247 $M_w = 3.0$ (based on the M_L to M_w correlation of Grünthal et al., 2009) and at least 50 macroseismic
248 intensity data points (IDPs) were included. The online BGS database currently only extends to the
249 year 2001. In addition to those events, five additional events were incorporated into the dataset for
250 this study, including Folkestone (4.0 M_w) and Market Rasen (4.5 M_w) events. Data for these
251 events were taken from the USGS “Did you feel it?” database. The database does not include the
252 Dudley, Ramsgate and Caernarfon events. Table 4 presents the main features of the included
253 earthquakes, while Figure 5 shows the geographical distribution of the epicentres.

254 An initial dataset of 15,3662 IDPs was compiled. Only IDPs from earthquakes with moment
255 magnitude greater than or equal to 3, epicentral distance lower than 300 km and an intensity value
256 greater than or equal to 3 were retained. The final dataset consists of a total of 11,412 IDPs. Since
257 intensity is a categorical variable, "half-levels" of intensity do not exist. When these are found,
258 generally displayed as for instance 3-4 or 5-6, the uncertainty in the intensity value is highlighted.
259 These values are usually lumped with integer levels before proceeding any further. In this study,
260 we randomly assigned each such IDP to the lower or higher level, with equal probability. The

261 initial and final datasets are presented in Figure 6 in terms of distributions of macroseismic
262 intensity versus distance.

263 **PRE-SELECTED GMPEs FOR THE UK**

264 As mentioned in the Introduction, the UK is a region of low seismicity for which strong motion
265 data are rare. Moreover, the absence of reliable modern GMPEs specific for the UK makes the
266 characterization of the ground motion attenuation for a seismic hazard assessment much more
267 complicated. Equations from other regions need to be adopted and sometimes adapted to the
268 regional conditions specific of the UK based on the limited available data.

269 Douglas (2018, Data and Resources) identifies a total of 450 published GMPEs which estimate
270 PGA and 290 published GMPEs which estimate elastic response spectral ordinates. Criteria for
271 the selection of GMPEs were first proposed by Cotton et al. (2006) and revisited by Bommer et al.
272 (2010). These two sets of authors provide a total of 10 criteria which could assist with the selection
273 of candidate GMPEs. Bommer et al. (2010) noted that only eight GMPEs met their criteria at the
274 time of their publication. These consist of four NGA-West (Next Generation Attenuation
275 Relationships for western US) GMPEs (Abrahamson and Silva, 2008; Boore and Atkinson, 2008;
276 Campbell and Bozorgnia, 2008; Chiou and Youngs, 2008), Akkar and Bommer (2010), Atkinson
277 and Boore (2006), Toro et al. (1997, modified as Toro, 2002) and Zhao et al. (2006). Since the
278 criteria were published, many new GMPEs have been developed, as well as updates to the NGA
279 West GMPEs.

280 Based on considerations of the UK characteristics, in addition to the criteria of Bommer et al.
281 (2010) the following points were considered:

- 282 - Models developed for shield regions were excluded since the geological processes which
283 led to the existence of the UK are significantly different to landmasses which exist today
284 due to the formation of a shield. These differences will lead to different attenuation
285 characteristics (Douglas, 2011);
- 286 - Only GMPE which incorporate an explicit V_{s30} term were included since κ_0 adjustments
287 are required to make GMPEs from elsewhere applicable to the UK low kappa-site values
288 shown in Figure 1 and to hard rock sites;
- 289 - Stochastic GMPEs based on Eastern North America (ENA) were excluded based on the
290 difference in the attenuation of the seismic waves (Figure 3).

291 Based on these considerations, the GMPEs that were not rejected are the NGA West 2 GMPEs
292 (Abrahamson et al., 2014, ASK14; Boore et al., 2014, BSSA14; Campbell and Bozorgnia, 2014,
293 CB14; Chiou and Youngs, 2014, CY14; and Idriss 2014, I14), Bindi et al. (2014), BI14, Akkar et
294 al. (2014a,b), ASB14, and Cauzzi et al., 2015, CA15. However, based on the limits of applicability
295 of the Idriss (2014) model ($M_w \geq 5$, $R \leq 150$ km and $V_{s30} \geq 450$ m/s) and the inconsistencies with
296 the available dataset for the UK earthquakes (Figure 5 and Figure 7), this GMPE was excluded
297 from the following analysis.

298 In addition to the above GMPEs, the GMPE of Rietbrock and Edwards (2017), RE17,
299 summarized in this paper is included. It is noted that although not yet published, the model is an
300 update of an already published model and therefore fulfils the criteria described in Bommer et al.
301 (2010). Moreover, although the model does not incorporate a V_{s30} term, it has been specifically
302 developed for hard rock sites in the UK, therefore no adjustment will be necessary when applied
303 to these conditions. In the following analysis, this GMPE is also compared against UK data that
304 do not lie on hard rock, showing a very good performance.

V_s-κ₀ ADJUSTMENT FACTORS FOR THE UK

305

306 The high frequency attenuation parameters of the candidate GMPEs, κ_{host} , were computed to
307 ensure these were consistent with the UK values (Figure 1) using the inverse random vibration
308 theory, iRVT (Gasparini and Vanmarcke, 1976). To this end, response spectra for a set of
309 magnitude and distance bins were computed, in particular M_w of 4.5, 5.5 and 6.5 and epicentral
310 distances R_{epi} of 5, 10 and 20 km were used. Table 6 shows average κ_{host} values computed in this
311 study for the selected empirical GMPEs. These values are larger than the average values for site
312 class found by RE17.

313 Therefore, prior to any statistical analysis, adjustment factors for the UK were determined to
314 modify the GMPEs for the average κ_0 values in the UK, following the methodology in PNNL
315 (2014). The parameters needed for the adjustment factors are usually (1) the definition of V_s
316 profiles and κ_0 values at the target site (i.e., a generic site in the UK) and (2) the definition of the
317 V_s profiles and κ_0 at the host location, i.e. the average rock site for the selected GMPE.

318 For stations on stiff soil or rock, the V_{s30} values are within the range of applicability of the
319 GMPEs, thus no adjustment for V_s was applied. The target high frequency parameter, κ_{target} , was
320 assumed as 0.03 s, as per Figure 1. The κ_{host} values are those from Table 6.

321 For hard rock station, adjustments both for the V_s profile and the κ value were required where
322 the target κ_0 value is taken as 0.012 s. The target V_s profile for the UK was defined according to
323 Booth et al. (2001). The κ_{host} values are those from Table 6 corresponding to a V_{s30} of 760 m/s.
324 The host V_s profiles for the empirical GMPEs were defined as follows:

325 - For all the NGA West GMPEs, the V_s profile defined by Boore (2015) was adopted.

326 - For the GMPEs of Akkar et al. (2014a,b) and Bindi et al. (2014), the V_s profile
327 corresponding to an average V_{S30} of 760 m/s was derived using available V_s profiles on
328 rock stations from Italy, Greece and Turkey (see Data and Resource), with a total of 13
329 stations.

330 - For the GMPE of Cauzzi et al. (2015), rock stations from the dataset with available V_s
331 profiles were used, which consisted of 16 V_s profiles from Kik-net dataset and two from
332 the Italian dataset (see Data and Resource).

333 The adjustment factors for the UK are shown in Figure 8 for three GMPEs. All the empirical
334 GMPEs are corrected using the V_s - κ_0 adjustment factors for the UK. No adjustments are applied
335 to the stochastic UK specific model.

336 The dependence of κ on magnitude, distance and V_{S30} was also explored. Results show a clear
337 trend with κ decreasing as V_{S30} increases: for low V_{S30} values (250 or 400 m/s), kappa shows a
338 stronger dependence on magnitude and distance compared with higher V_{S30} values. All the GMPEs
339 showed similar trends.

340 **COMPARISON OF GMPES WITH THE UK DATA**

341 **COMPARISON WITH THE UK INSTRUMENTAL GROUND MOTION DATA**

342 Comparisons of the attenuation curves from the nine preselected GMPEs and the observations
343 from the Dudley, Folkestone, Market Rasen and Swansea earthquakes are shown in Figure 9 and
344 Figure 10. The attenuation curves are computed for sites with a V_{S30} of 760 m/s in the empirical
345 GMPEs. The stations on rock, which are comparable with the curves, are shown as white squares.
346 All other observations are shown, for completeness, as gray circles. In general, the predictions
347 from the GMPEs slightly under-predict the observations from the Market Rasen earthquake which

348 has been formulated by several authors that could be a high stress drop event (e.g. Sargeant and
349 Ottömoller, 2010). Good agreement is found for the other three earthquakes. For the GMPEs of
350 RE17 the white squares represent data on hard rock sites consistent with the attenuation curves
351 specific for hard rock sites. The agreement is very good for all four earthquakes.

352 There are numerous statistical methods to test the agreement between observed and predicted
353 data (e.g. Chi-square test, Kolmogorov-Smirnov test, variance reduction and Pearson's correlation
354 coefficient). These statistical methods can be used to understand the suitability of a given
355 predictive model under a set of collected ground motions. A brief description of these methods can
356 be found in Kale and Akkar (2013).

357 In this study, three methods are discussed to quantitatively evaluate the performance of the
358 preselected GMPEs with respect to the UK dataset: the classical residual analysis, the method
359 proposed by Scherbaum et al. (2009) and the method proposed by Kale and Akkar (2013).

360 The most common methodology for assessing predictive model performance is the residual
361 analysis. This statistical method determines the existence of bias through the application of mean
362 residuals, as well as the trend of the total residuals as function of estimator parameters such as
363 magnitude and source to site distance.

364 The normalized residuals can be calculated as:

$$365 \quad \text{residual}(f) = \frac{\log(\text{obs}(f)) - \log(\text{pre}(f))}{\sigma_{\text{GMPE}}(f)} \quad (6)$$

366 where residual is the total normalized residual at the spectral frequency, f , $\text{obs}(f)$ and $\text{pre}(f)$ are
367 the observed and predicted spectral accelerations respectively and $\sigma_{\text{GMPE}}(f)$ is the total standard
368 deviation of the model at a given spectral frequency. A positive value indicates that the observed
369 ground motions are larger than those predicted by the GMPE while a negative value of the residual

370 indicates that the observed ground motions are lower than the predictions (i.e. the model over-
371 predicts the data).

372 Residuals were computed for 10 spectral frequencies between 0 and 3 s. Figure 11 and Figure
373 12 show the residuals (gray circles) in terms of magnitude and distance for each of the preselected
374 GMPEs for the PGA and the spectral acceleration at 1 s. The white squares in the figures show the
375 average values for magnitude and distance intervals, in order to highlight if a clear trend exists.
376 The comparisons show that most of the residuals fall within three standard deviations. Calculated
377 residuals for some of the equations indicate under prediction of the observed ground motions (e.g.
378 Boore et al., 2014; and Campbell and Bozorgnia, 2014).

379 Table 7 presents a qualitative summary of the general performance of the GMPEs. Overall, the
380 GMPEs slightly under-predict the data. Considering only the data within 100 km of the earthquake
381 sources, the mean residuals for the different frequencies tested are either side of zero or very close
382 to zero, indicating reasonable performance for many of the GMPEs. Although the GMPE of for
383 Cauzzi et al. (2015) GMPE is defined for a minimum magnitude M_w of 4.5, it performs well
384 against the UK data.

385 To have a better understanding of the performance of the GMPEs against the UK recorded
386 data, statistical tests were also investigated. The method proposed by Scherbaum et al. (2009)
387 attempts to overcome the limitations found in the previous method by Scherbaum et al. (2004).
388 Scherbaum et al. (2004) proposed a scheme based on exceedance probabilities (or likelihood, LH,
389 values) to quantify the appropriateness of candidate models with respect to a set of response
390 spectral reference data. One of the shortcomings of their method is that it still requires subjective
391 decisions (e.g. definition of classes and thresholds for acceptability). Although the LH method was
392 proven to be a robust approach for ranking the candidate GMPEs, its dependence on data size and

393 subjectivity in choosing the threshold LH value, led Scherbaum et al. (2009) to propose the log
394 likelihood (LLH) method that overcomes these limits. The authors proposed an information
395 theoretic approach that is more general and does not depend on ad hoc assumptions.

396 The method computes the log likelihood parameter which is defined as:

$$397 \quad LLH(g, \underline{x}) = -\frac{1}{N} \sum_{i=1}^N \log_2(g(x_i)) \quad (7)$$

398 where $x=\{x_i\}$, $i = 1 \dots N$ are the empirical data and $g(x_i)$ is the probability density function given
399 by a GMPE to predict the observation x_i .

400 Since LLH is a divergence criterion to rank the candidate GMPEs, a small LLH indicates that
401 the candidate model is close to representing the process that has generated the data while a large
402 LLH corresponds to a model that is less likely of representing the observed data well.

403 Arroyo et al. (2014) highlight that the method may lead to incorrect weightings although
404 correct ranking of models. In this study, we only use the LLH method for ranking the candidate
405 GMPEs.

406 Kale and Akkar (2013) noted that the method proposed by Scherbaum et al. (2009) focuses on
407 selecting a suite of GMPEs that can accurately represent the aleatory variability of the ground
408 motion dataset used in testing. This objective may favor GMPEs with large sigma and selection of
409 such GMPEs may result in conservative probabilistic seismic hazard for low annual probabilities
410 of exceedance (Restrepo-Velez and Bommer, 2003). The authors propose a different metric
411 (instead of likelihood) that tends to use greater weight for increased closeness to the mean value
412 of the model and less weight for the impact of outliers. The method is based on the Euclidean
413 distance which separately considers ground motion uncertainty (i.e. aleatory variability addressed

414 by the standard deviation) and the bias between the observed data and median estimations of
415 candidate GMPEs. Three indices are obtained from this method:

- 416 - The normalized distance based ranking (MDE), which evaluates the effect of sigma
417 while testing the performance of the GMPE under a given ground motion database;
- 418 - $k_{0.5}$, which provides the performance of the median prediction from the GMPE. The
419 parameter k is the ratio of the original and corrected Euclidean distances. Therefore, it
420 occurs when the estimates from the GMPEs are very close to the observations. The
421 optimum value is 1; and
- 422 - Euclidean distance based ranking (EDR), which provides an estimate of the overall
423 performance of the model.

424 Detailed equations for this method are provided in Kale and Akkar (2013).

425 Mak et al. (2014) criticized the method, in particular the index MDE, which according to the
426 authors, favors a smaller modeled uncertainty when two predictions give the same mean. However,
427 in their reply Kale and Akkar (2014) explains that MDE is tailored to assess the influence of GMPE
428 sigma on the estimated ground motions, while larger differences between the observed data and
429 estimated median will be penalized by $k_{0.5}$. Moreover, the authors highlight that EDR, as a two-
430 component score, would not prefer a model in which the median estimates entirely disagree with
431 the observed data.

432 Figure 13 shows the results of the eight preselected GMPEs in terms of LLH values with
433 frequency while Figure 14 provides the results of the method by Kale and Akkar (2013).

434 Table 8 summarized the results providing the average score over the range of periods
435 considered in the Scherbaum et al. (2009) and Kale and Akkar(2013) statistical tests. To assist the

436 reader, the three GMPEs that performed the best are underlined: Abrahamson et al. (2014), Cauzzi
437 et al. (2015) and Rietbrock and Edwards (2017).

438 COMPARISON WITH THE UK MACROSEISMIC DATA

439 Due to a lack of strong motion data at short distances and larger magnitudes, a macroseismic
440 dataset for the UK was also used to test the nine preselected GMPEs. This allows inclusion of
441 earthquakes with magnitude greater than 4.0Mw and greatly increases the number of data close to
442 the epicentre of an earthquake. The idea of using macroseismic data to evaluate the performance
443 of GMPEs was proposed by Scherbaum et al. (2009) who demonstrated it to be a useful way of
444 assessing GMPEs using Californian data from Delavaud et al. (2009).

445 The methodology is similar to that used for UK instrumental data. However, an additional step
446 is required, involving conversion of the PGA ground motion into a macroseismic intensity.
447 Therefore, an assessment of a correlation between ground motion and intensity needs to be
448 undertaken. A total of six relationships were considered and are presented in Table 9.

449 To test their applicability, the correlations were compared for seven earthquakes in the UK for
450 which both recorded PGA and macroseismic intensities were available: Penzance, Arran,
451 Sennybridge, Warwick, Dudley, Folkestone and Market Rasen. For all events intensity
452 observations at the recording stations were assigned based on the intensity maps or an interpolation
453 of the closest intensity measurements. For each relationship, the median and its 5-95% band of
454 variability are compared with the data in Figure 15. Although the uncertainty of the relationship
455 between ground motion and intensity is large, the two correlations that best capture the UK data
456 are: (1) Faccioli and Cauzzi (2006), FC06, based on a dataset with distances lower than 100 km
457 and PGA values between 0.2 and 6 m/s² and (2) Atkinson and Kaka (2007), AK07, which also

458 includes earthquakes at very large distances; up to about 500 km. Both equations are of the form:

459 $I_{EMS} = a + b \log PGA$ with an associated uncertainty σ_{GMICE} .

460 For the computation of the residuals equation (1) was modified as below:

461
$$\text{residual} = \frac{I_{\text{obs}} - I_{\text{pre}}}{\sigma_I} \quad (8)$$

462 where I_{obs} is the observed macroseismic intensity, I_{pre} is the predicted value derived from the
463 conversion of the predicted PGA from the GMPE and σ_I is the standard error associated with the
464 prediction. Since the PGA comes from a GMPE and therefore has an associated standard error, the
465 total standard error was computed as shown below:

466
$$\sigma_I = \sqrt{(b \sigma_{\log_{10}(PGA)})^2 + \sigma_{GMICE}^2} \quad (9)$$

467 where $\sigma_{\log_{10}(PGA)}$ is the standard error of the logarithm of PGA in base 10.

468 To allow the comparison of GMPEs with the macroseismic data, an estimate of V_{S30} at each
469 macroseismic location is required. An estimate of V_{S30} was obtained using the global V_{S30} maps
470 provided by the USGS (Wald and Allen 2007), based on correlations between topography and
471 V_{S30} . Although the method has recognized limitations, it has been used for this study only to assess
472 the V_{S30} at the macroseismic locations due to the large amount of data to be processed and the
473 scarcity of information on the V_{S30} parameter over the whole of the UK. Linear interpolation from
474 the Wald and Allen (2007) map was adopted.

475 Examples of the results in terms of residuals is presented in Figure 15 for the GMPE of
476 BSSA14, BI14 and CA15 using the correlation of Faccioli and Cauzzi (2006). Similar trends in
477 the residuals are found using Atkinson and Kaka (2007).

478 In general, the trend of the residuals does not differ from that found for the ground motion data
479 at short period. The residuals with respect to magnitude are close to zero for $M_w \geq 4$ in the case of
480 Abrahamson et al. (2014) and Chiou and Youngs (2014). A slight under prediction is found in the
481 case of Bindi et al. (2014), Campbell and Bozorgnia (2014), Cauzzi et al. (2015) and Rietbrock
482 and Edwards (2017), while Akkar et al. (2014) display strong linear trends.

483 The results in terms of the two methods of Scherbaum et al. (2009) and Kale and Akkar (2013)
484 are presented in Table 10 where the three best results for each test are underlined. Overall,
485 Abrahamson et al. (2014), Boore et al. (2014), Chiou and Youngs (2014), Cauzzi et al. (2015) and
486 the stochastic UK specific model, Rietbrock and Edwards (2017) show good performance.

487 **COMPARISON OF GMPEs' MEDIAN PREDICTION**

488 The approach used to evaluate similarities in the GMPEs involved the graphical comparison of
489 the attenuation curves (e.g. PGA versus distance) for a particular magnitude value and spectral
490 ordinate. Figure 17 shows comparisons among the response spectra computed with eight GMPEs
491 adopted in this study for hard rock sites, for two moment magnitude (5 and 6) and two epicentral
492 distances (15 and 50 km). For the conversion among the different distance metrics a strike slip
493 fault mechanism (typical for UK earthquakes) has been assumed in all cases. The figure
494 highlights the differences among the GMPEs in terms of predicted amplitude and spectral shape.
495 The Rietbrock and Edwards (2017) appears as the most dissimilar. The level of amplitudes
496 predicted is overall comparable, however the peak of the spectrum occurs at 0.1 s while for the
497 empirical adjusted GMPEs it is found at 0.05 s. Moreover, the spectral accelerations are lower
498 than the other GMPEs at very short period, and much larger at periods longer than 0.1 s
499 especially for a distance of 50 km. Among the empirical adjusted GMPEs, ASK14 provides the
500 larger acceleration at magnitude 5.

501 An exhaustive comparison of all the GMPEs for many spectral periods and magnitudes is not
502 practical and would be difficult to evaluate in an objective manner. To overcome this issue,
503 Scherbaum et al. (2010) suggest the use of the Sammon's maps (Sammon, 1969). Sammon's
504 maps are a statistical technique which enables the projection of high dimensional vectors onto
505 2D maps in such a way that the distances between the vectors can be preserved. More than one
506 2D configuration can exist for a given set of GMPEs. The absolute numbers on the axes do not
507 have a physical meaning. Only the distances and relative positions are of importance.

508 Given the spectral acceleration, SA, for a certain magnitude distance combination k, the
509 Euclidean distance $\Delta GMPE_{ij}$ between two GMPEs, i and j is computed as:

$$510 \quad \Delta GMPE_{ij} = \sqrt{\sum_k (\log SA_{k,i} - \log SA_{k,j})^2} \quad (10)$$

511 and projected in 2D maps. In this study, the Euclidean distances were computed based on
512 magnitudes between 4.0 to 7.0 Mw at 0.2 Mw intervals for 12 R_{epi} distances (1, 5, 10, 20, 30...
513 100 km). For each combination of magnitude and distance, the ground motion has been
514 computed at periods between 0 and 3 s. Examples of the results are shown in Figure 18 for rock
515 (where RE17 is not included) and in Figure 19 for hard rock (where all the GMPEs are corrected
516 for a κ_0 of 0.012s, except RE17 which is directly applicable on hard rock). Maps of the
517 Euclidean distances for each spectral ordinate are also presented and shown on the left panels of
518 the figures. Dark colours highlight the GMPEs that are most dissimilar. Of the four NGA West 2
519 GMPEs, Abrahamson et al. (2014) and Chiou and Youngs (2014) are relatively close, indicating
520 that the two provide similar predictions, while Boore et al. (2014) and Campbell and Bozorgnia
521 are more distant from the others. Also, Akkar et al. (2014) and Bindi et al. (2014) are relatively

522 close at all spectral periods. Large distances are found between the Rietbrock and Edwards
523 (2017) and all adjusted empirical GMPEs when the predictions are used for hard rock sites.

524 **DISCUSSION AND CONCLUSIONS**

525 In region of high seismicity, the definition of the ground motion attenuation can often benefit
526 from the availability of a large number of instrumentally recorded ground motion data that cover
527 the magnitude and distance ranges of interest of a seismic hazard assessment and, as a
528 consequence, of published ground motion prediction equations developed specifically for the same
529 region. This becomes more complicated when the site under study is in a region of low-to-moderate
530 seismicity. Generally, available time histories are scarce and many times they are related to low or
531 moderate magnitude earthquakes. This is the case of the UK, where the maximum magnitude of
532 the instrumentally recorded ground motion data is $M_w = 4.5$ (related to the Market Rasen
533 earthquake occurred in 2008). This study attempts to select GMPEs through a methodic approach
534 that compares the predictions from GMPEs available from elsewhere against available UK data.
535 A UK instrumental dataset was firstly collated and used for comparison against the GMPEs
536 prediction. It is highlighted that the dataset in statistical terms has sufficient data to perform
537 statistical tests and the data are consistent with the datasets of the GMPEs. However, the
538 extrapolation of the results for magnitude lower than 4.5 to larger magnitude can be difficult.
539 Therefore, given the scarcity of instrumental data especially for magnitude greater than 4.5, the
540 study proposes to make use also of macroseismic observations. The uncertainty related to the
541 conversion from intensity and ground motion (in this case PGA) was carried through the
542 calculations and combined with the uncertainty in the estimation of PGA from the GMPEs.

543 The empirical GMPEs selected based on Bommer et al. (2010) from other parts of the world
544 required adjustments in order to account for specific characteristics of the attenuation of the ground

545 motion in the UK. In this study, a correction between the kappa-site from the GMPE (κ_{host}) and
546 kappa-site values specifically computed for the UK stations was applied prior to any comparison.
547 Therefore, all the comparisons and analyses were performed with adjusted empirical GMPEs. A
548 correction for the quality factor attenuation was not considered, although this could be a possible
549 improvement. However, the comparison between the Q_{Lg-1} attenuation between the UK and West
550 US presented in Figure 3 showed that differences are small. In addition to empirical GMPEs, an
551 update of the stochastic model of Rietbrock et al. (2013) was developed within the study and herein
552 referred to as Rietbrock and Edwards (2017). The GMPE is for hard rock sites in the UK. A total
553 of eight GMPEs were used in the analyses.

554 Based on the residuals analysis, the statistical results computed with Scherbaum et al. (2009)
555 and Kale and Akkar (2013) and the Sammon's maps, the following observations are made:

- 556 - The Rietbrock and Edwards (2017) GMPE performs very well against instrumental
557 and macroseismic data also for sites that are not classified as hard rock. It behaves
558 differently from all the other GMPEs in terms of median prediction at all periods;
- 559 - The four NGA West2 GMPEs are based on the same, or similar, dataset and were
560 developed within the same project. Comparisons against UK data showed that the
561 GMPE developed by Campbell and Bozorgnia (2014) is the one that worse fits the data,
562 while the GMPE by Abrahamson et al. (2014) and Chiou and Youngs (2014) displayed
563 a better fit with the UK data. The Sammon's maps showed that Abrahamson et al.
564 (2014) and Chiou and Youngs (2014) are expected to perform similarly, while among
565 these four GMPEs, Boore et al. (2014) shows larger distances.

566 - Bindi et al. (2014) and Akkar et al. (2014a, b) are both based on European data and in
567 the Sammon's maps they appear to perform in a similar way at short period. Among
568 the two GMPEs, Bindi et al. (2014) performed better against the UK data.

569 - The predictions from Cauzzi et al. (2015) are in agreement with the UK data and they
570 are distant on the Sammon's maps with respect to the other GMPEs. However, for some
571 spectral periods, they are close in the Sammon's maps to Chiou and Youngs (2014).
572 However, their datasets are completely independent and based mainly on two different
573 regions: California and Japan.

574 This study shows that five empirical GMPEs adjusted for the UK kappa-site values provide
575 predictions that are consistent with the UK data: Abrahamson et al. (2014), Chiou and
576 Youngs (2014), Boore et al. (2014), Bindi et al. (2014) and Cauzzi et al. (2015).

577 Given the lack of instrumental recorded data for magnitude greater than 4.5, and therefore
578 the uncertainty on the spectral shape of future earthquakes, the use of multiple GMPEs is
579 recommended. Based on the results and the GMPEs similarities in terms of database, it is
580 recommended that in the definition of the ground motion characterization for a PSHA in
581 the UK, at least one NGA West 2 GMPE among the above three is selected together with
582 the GMPEs of Bindi et al. (2014) and Cauzzi et al. (2015). For PSHA on hard rock sites,
583 in addition to the above GMPEs adjusted for the appropriate V_s - κ_0 , Rietbrock and Edwards
584 (2017) is recommended as, this analysis shows a very good agreement well with the UK
585 ground motion data.

586

587
588
589
590
591
592
593
594
595
596
597
598
599
600
601
602
603
604
605
606

DATA AND RESOURCES

- Ground motion data were made available to the authors directly by the British Geological Survey (BGS).
- Macroseismic data were downloaded from the Historical Earthquake Database from the BGS website: <http://quakes.bgs.ac.uk/historical/>. Last accessed February 2016
- V_{s30} data for the UK were downloaded from: Global VS30 Map Server, retrieved from earthquake.usgs.gov/hazards/apps/vs30/, Last accessed December 2015.
- List of available GMPEs until 2015 were consulted from Douglas, J. (2015). Ground motion prediction equations 1964 – 2015, <http://www.gmpe.org.uk>, Last accessed February 2016
- V_s profiles for stations in Italy were retrieved from the ITACA (Italian Accelerometric Archive) Project (available at <http://itaca.mi.ingv.it>), Last accessed February 2016
- V_s profiles for stations in Greece were retrieved from the database monitored by ITSAK (Institute of Engineering Seismology and Earthquake Engineering) <http://monographs.itsak.gr/>. Last accessed February 2016.
- V_s profiles for stations in Turkey were retrieved from the database of the Disaster and Emergency Management Presidency of Turkey (<http://kyh.deprem.gov.tr/en/home>). Last accessed February 2016.
- V_s profiles for stations in Japan were retrieved from the Kik-Net website (<http://www.kyoshin.bosai.go.jp/>). Last accessed February 2016.

607

ACKNOWLEDGMENTS

608 This research was sponsored by Horizon Nuclear Power. Any statements, opinions, findings,
609 conclusions or recommendations expressed in this material are those of the authors and do not
610 necessarily reflect those of the funding or sponsoring agency. The authors are grateful to Dr. Roger
611 Musson for the useful discussions throughout the Wylfa Newydd project.

612

REFERENCES

- 613 Abrahamson, N. A. and Silva, W. J. (2008). Summary of the Abrahamson and Silva NGA ground-
614 motion relations. *Earthquake Spectra*, vol. 24, no. 1, p. 67-97.
- 615 Abrahamson, N. A., Silva, W. J. and Kamai, R. (2014). Summary of the ASK14 ground motion
616 relation for active crustal regions. *Earthquake Spectra*, 30(3):1025–1055.
- 617 Akkar, S. and Bommer, J. J. (2010). Empirical Equations for the Prediction of PGA, PGV, and
618 Spectral Accelerations in Europe, the Mediterranean Region, and the Middle East,
619 *Seismological Research Letters*, 81, 195-206.
- 620 Akkar, S., Sandikkaya, M. A. and Bommer, J. J. (2014a). Empirical ground-motion models for
621 point- and extended-source crustal earthquake scenarios in Europe and the Middle East.
622 *Bulletin of Earthquake Engineering*, 12(1):359–387
- 623 Akkar, S., Sandikkaya, M. A. and Bommer, J. J. (2014b). Erratum to: Empirical ground-motion
624 models for point- and extended-source crustal earthquake scenarios in Europe and the Middle
625 East. *Bulletin of Earthquake Engineering*, 12(1):389–390
- 626 Anderson, J. G. and Hough, S. E. (1984). A model for the shape of the Fourier amplitude spectrum
627 of acceleration at high frequencies, *Bull. Seismol. Soc. Am.* 74, no. 5, 1969-1993.

628 Arroyo, D., Ordaz, M., Rueda, R. (2014) On the Selection of Ground-Motion Prediction Equations
629 for Probabilistic Seismic-Hazard Analysis. *Bulletin of the Seismological Society of America*,
630 104 (4): 1860–1875

631 Arup (1993). Earthquake hazard and risk in the UK. Report prepared for the Department of the
632 Environment, pp 315.

633 Atkinson, G. M. and Boore, D. M. (2006). Earthquake ground-motion prediction equations for
634 eastern North America. *Bulletin of the Seismological Society of America* 96(6), 2181-2205.

635 Atkinson, G. M. and Kaka, S. I. (2007). Relationships between felt intensity and instrumental
636 ground motion in the Central United States and California, *Bulletin of the Seismological*
637 *Society of America*, 97(4), 1350–1354.

638 Baptie, B., Ottemöller, L., Sargeant, S., Ford, G. and O’Mongain, A. (2005). The Dudley
639 earthquake of 2002: a moderate sized earthquake in the UK. *Tectonophysics* 401(1), 1-22.

640 Bindi, D., Massa, M., Luzi, L., Ameri, G., Pacor, F., Puglia, R. and Augiera, P. (2014). Pan-
641 European ground-motion prediction equations for the average horizontal component of PGA,
642 PGV, and 5%-damped PSA at spectral periods up to 3.0 s using the RESORCE dataset. *Bull*
643 *Earthquake Eng.* Doi:10.1007/s10518-013-9525-5

644 Bommer, J. J., Douglas, J., Scherbaum, F., Cotton, F., Bungum, H. and Fäh, D. (2010). On the
645 Selection of Ground-Motion Prediction Equations for Seismic Hazard Analysis. *Seismological*
646 *Research Letters* Volume 81, Number 5, pp783-793.

647 Bommer, J. J., Coppersmith K. J., Coppersmith R. T., Hanson, K. L., Mangongolo, A., Neveling,
648 J., Rathje, E. M., Rodriguez-Marek, A., Scherbaum, F., Shelembed, R., Stafford, P. J. and
649 Strasser, F. O. (2015). A SSHAC Level 3 Probabilistic Seismic Hazard Analysis for a New-

650 Build Nuclear Site in South Africa. *Earthquake Spectra*, Vol:31, ISSN:8755-2930, Pages:661-
651 698.

652 Boore, D. M. (2015). Determining generic velocity and density models for crustal amplification
653 calculations, with an update of the Boore and Joyner (1997) generic site amplification for
654 $V_s(Z) = 760\text{m/s}$. *Bulletin of the Seismological Society of America*, Vol. 106, No. 1, pp. 316–
655 320, February 2016, doi: 10.1785/0120150229.

656

657 Boore, D. M. (2003). Simulation of Ground Motion Using the Stochastic Method. *Pure and*
658 *Applied Geophysics*, 160, 635-676.

659 Boore, D. M. and Atkinson, G. M. (2008). Ground-motion prediction equations for the average
660 horizontal component of PGA, PGV, and 5%-damped PSA at spectral periods between 0.01 s
661 and 10.0 s: *Earthquake Spectra*, vol. 24, no. 1, p. 99-138.

662 Boore, D. M. and Thompson E. M. (2014). Path durations for use in the stochastic-method
663 simulation of ground motions, *Bulletin of the Seismological Society of America*. Vol. 104, No.
664 5, pp. 2541-2552

665 Boore, D. M., Stewart, J. P., Seyhan, E. and Atkinson, G. M. (2014) NGA-West 2 equations for
666 predicting PGA, PGV, and 5%-damped PSA for shallow crustal earthquakes. *Earthquake*
667 *Spectra*, 30(3):1057–1085.

668 Borchedt, R. D. (1994), Estimates of site-dependent response spectra for design (Methodology and
669 Justification), *Earthquake Spectra*, Vol. 10(4), pp. 617-653.

670 Booth, D., Bott, J. and O’Mongain, A. (2001). The UK seismic velocity model for earthquake
671 location—a baseline review, Internal Report IR/01/188, British Geological Survey, Edinburgh,
672 United Kingdom.

673 Campbell, K. W. and Bozorgnia, Y. (2008). NGA ground motion model for the geometric mean
674 horizontal component of PGA, PGV, PGD and 5% damped linear elastic response spectra for
675 periods ranging from 0.01 to 10 s. *Earthquake Spectra*, vol. 24, no. 1, p. 139-171.

676 Campbell, K. W. and Bozorgnia, Y. (2014). NGA-West 2 ground motion model for the average
677 horizontal components of PGA, PGV, and 5%-damped linear acceleration response spectra.
678 *Earthquake Spectra*, 30(3): 1087–1115.

679 Cauzzi, C., Faccioli, E., Vanini, M. and Bianchini, A. (2015). Updated predictive equations for
680 broadband (0.01–10s) horizontal response spectra and peak ground motions, based on a global
681 dataset of digital acceleration records. *Bulletin of Earthquake Engineering*, Vol 13, pp 1587-
682 1612.

683 Chiou, B. S-J. and Youngs, R. R. (2008). An NGA model for the average horizontal component
684 of peak ground motion and response spectra. *Earthquake Spectra*, vol. 24, no. 1, p. 173-215.

685 Chiou, B. S-J. and Youngs, R. R. (2014). Update of the Chiou and Youngs NGA model for the
686 average horizontal component of peak ground motion and response spectra. *Earthquake*
687 *Spectra*, 30(3):1117–1153.

688 Christensen, N. I., Wilkens, R. H., Blair, S. C. and Carlson, R. L. (1980), Initial Reports of the
689 Deep Sea Drilling Project, Volume LIX, Washington, Chapter 10. Reprinted from Kroenke,
690 L., Scott, R., et al., 1980. http://deepsedrilling.org/59/volume/dsdp59_10.pdf

691 Cotton, F., Scherbaum, F., Bommer, J. J. and Bungum H. (2006). Criteria for selecting and
692 adjusting ground-motion models for specific target applications: Applications to Central
693 Europe and rock sites. *Journal of Seismology*, Vol 10 (2), pp137-156

694 Delavaud, E., Scherbaum, F., Kuehn, N. and Riggelsen, C. (2009). Information-Theoretic
695 Selection of Ground-Motion Prediction Equations for Seismic Hazard Analysis: An

696 Applicability Study Using California Data, *Bulletin of the Seismological Society of America*,
697 Vol. 99, No. 6, pp. 3248-3263.

698 Di Alessandro, C., Bonilla, L. F., Boore, D. M., Rovelli, A. and Scotti, O. (2012). Predominant-
699 period site classification for response spectra prediction equations in Italy. *Bulletin of the*
700 *Seismological Society of America*, 102(2):680–695.

701 Douglas, J. (2011). Investigating possible regional dependence in strong ground motions. in
702 "Earthquake Data in Engineering Seismology", Sinan Akkar, Polat Gülkan, Torild van Eck
703 (Ed.), 29-38.

704 Edwards, B., Rietbrock, A., Bommer, J. J. and Baptie, B. (2008). The acquisition of source, path
705 and site effects from Microearthquake Recordings Using Q Tomography: Application to the
706 United Kingdom. *Bulletin of the Seismological Society of America*, 98, 1915-1935.

707 Faccioli, E. and Cauzzi, C. (2006). Macroseismic intensities for seismic scenarios, estimated from
708 instrumentally based correlations, in *Abstract Book1st ECEES*,
709 http://www.ecees.org/abstracts_book.pdf, p. 125

710 Faenza, L. and Michelini, A. (2009), Regression analysis of MCS intensity and ground motion
711 parameters in Italy and its application in ShakeMap. *Geophysical Journal International*, 180:
712 1138–1152.

713 Gasparini, D. A. and Vanmarcke, E. H. (1976). Simulated earthquake motions compatible with
714 prescribed response spectra, Cambridge Massachusetts, Massachusetts Institute of
715 Technology.

716 Goda, K., Aspinall, W. and Taylor, C. A. (2013). Seismic hazard analysis for the U.K. Sensitivity
717 to spatial seismicity modelling and ground motion prediction equations. *Seismological*
718 *Research Letters*, Vol 84, No. 1, 112-129.

719

720 Grünthal, G., Wahlström, R. and Stromeyer, D. (2009). The unified catalogue of earthquakes in
721 central, northern, and northwestern Europe (CENEC) - updated and expanded to the last
722 millennium. *Journal of Seismology*, 13, 4, 517-541.

723 Idriss, I. M. (2014). An NGA-West 2 empirical model for estimating the horizontal spectral values
724 generated by shallow crustal earthquakes. *Earthquake Spectra*, 30(3):1155–1177.

725 Kale, Ö. and Akkar S. (2013) A New Procedure for Selecting and Ranking Ground-Motion
726 Prediction Equations (GMPEs): The Euclidean Distance-Based Ranking (EDR) Method,
727 *Bulletin of the Seismological Society of America*, Vol. 103(2A), pp. 1069–1084

728 Kale, Ö. and Akkar S. (2014). Reply to “Comment on ‘A New Procedure for Selecting and
729 Ranking Ground-Motion Prediction Equations (GMPEs): The Euclidean Distance-Based
730 Ranking (EDR) Method’ by Özkan Kale and Sinan Akkar” by Sum Mak, Robert Alan
731 Clements, and Danijel Schorlemmer, *Bulletin of the Seismological Society of America*, Vol.
732 104, No. 6, pp. 3141–3144

733 Mak, S., Clements, R. A. and Schorlemmer, D. (2014). Comment on “A New Procedure for
734 Selecting and Ranking Ground-Motion Prediction Equations (GMPEs): The Euclidean
735 Distance-Based Ranking (EDR) Method” by Özkan Kale and Sinan Akkar, *Bulletin of the*
736 *Seismological Society of America*, Vol. 104, No. 6, pp. 3139–3140.

737 Ottemöller, L. and Sargeant, S. (2010). Ground-Motion Difference between Two Moderate-Size
738 Earthquakes in the UK. *Bulletin of the Seismological Society of America*; August 2010; v.
739 100; no. 4; p. 1823-1829.

740 Ottemöller, L. Baptie, B., Smith, N.J.P. (2009). Source Parameters for the 28 April 2007 Mw 4.0
741 Earthquake in Folkestone, United Kingdom, *Bulletin of the Seismological Society of America*,
742 Vol. 99, No. 3, pp. 1853–1867

743 Pacific Northwest National Laboratory (PNNL) (2014). Hanford Sitewide Probabilistic Seismic
744 Hazard Analysis, prepared for the U.S. Department of Energy.

745 PML (1988). UK Uniform Risk Spectra. Report by Principia Mechanica Ltd for NNC, No 498/88.

746 Restrepo-Velez, L. F. and Bommer J. J. (2003). An exploration of the nature of the scatter in
747 ground-motion prediction equations and the implications for seismic hazard assessment, *J.*
748 *Earthq. Eng.* 7, no. S11, 171–199.

749 Rietbrock, A., Strasser, F. O. and Edwards, B. (2013). A stochastic earthquake ground motion
750 prediction model for the United Kingdom. *Bulletin of the Seismological Society of America*,
751 Vol 103(1), 57-77.

752 Rietbrock, A. and Edwards, B. (2017). Wylfa Seismic Hazard Consultancy Project, June 2017,
753 University of Liverpool, Leo Ref: 1619&2082, Version 2.3, Revision 08/06/2017.

754 Sammon, J.W. Jr (1969). A Nonlinear Mapping for data Structure Analysis. *IEEE Transactions on*
755 *Computers*, Vol C-18(5), pp. 401-409.

756 Sargeant, S. and Ottemöller, L. (2009). Lg wave attenuation in Britain. *Geophys. J. Int.*, 179, 1593–
757 1606.

758 Sargeant, S. L., Stafford, P. J., Lawley, R., Weatherill, G., Weston, A.-J. S., Bommer, J. J., Burton,
759 P. W., Free, M., Musson, R. M. W., Kuuyuur, T. and Rossetto, T. (2008). Observations from
760 the Folkestone, U.K., earthquake of 28 April 2007. *Seismological Research Letters* 79(5), 672-
761 687.

762 Scherbaum, F., Cotton, F. and Smith, P. (2004). On the use of response spectral-reference data for
763 the selection and ranking of ground-motion models for seismic-hazard analysis in regions of
764 moderate seismicity: The case of rock motion, *Bull. Seismol. Soc. Am.* 94, no. 6, 2164–2185

765 Scherbaum, F., Delavaud, E. and Riggelsen, C. (2009). Model selection in seismic hazard analysis:
766 An information–theoretic perspective, *Bull. Seismol. Soc. Am.* 99, no. 6, 3234–3247

767 Scherbaum, F., Kuehn, N. M., Ohrnberger, M. and Koehler, A. (2010) Exploring the Proximity of
768 Ground-Motion Models Using High-Dimensional Visualization Techniques. *Earthquake*
769 *Spectra*, Vol. 26, No. 4, pp. 1117-1138.

770 SHWP (2001). Uniform Risk Spectra for Wylfa Power Station. Report for Magnox Electric plc,
771 Seismic Hazard Working Party, Berkeley.

772

773 Tallet-Williams, S. and Fenton, C. (2015). A review of the development of VS30 ground profiles
774 for UK strong ground motion instrument sites. *SECED 2015 Conference: Earthquake Risk and*
775 *Engineering towards a Resilient World*, 9-10 July 2015, Cambridge UK.

776 Toro, G. R. (2002). Modification of the Toro et al. (1997) attenuation equations for large
777 magnitudes and short distances.

778 Toro, G. R., Abrahamson, N. A. and Schneider, J. F. (1997). Model of strong ground motions from
779 earthquakes in central and eastern North America: Best estimates and uncertainties.
780 *Seismological Research Letters* 68 (1), 41-57.

781 Tselentis, G. A. and Danciu, L. (2008). Empirical relationships between modified mercalli
782 intensity and engineering ground-motion parameters in Greece, *Bull. Seism. Soc. Am.*, 98(4),
783 1863–1875.

784 Wald, D. J. and Allen, T. I. (2007). Topographic Slope as a Proxy for Seismic Site Conditions and
785 Amplification. *Bulletin of the Seismological Society of America*, Vol. 97, No. 5, pp. 1379-
786 1395.

787 Wald, D. J., Quitoriano, V., Heaton, T. H. and Kanamori, H. (1999). Relationships between peak
788 ground acceleration, peak ground velocity, and Modified Mercalli intensity in California,
789 *Earthq. Spectra*, 15(3), 557–564.

790 Worden, C. B., Gerstenberger, M. C. Rhoades, D. A. and Wald, D. J. (2012). Probabilistic
791 Relationships between Ground-Motion Parameters and Modified Mercalli Intensity in
792 California. *Bulletin of the Seismological Society of America*, 102:1, pp. 204–221.

793 Zhao, J. X., Zhang, J., Asano, A., Ohno, Y., Oouchi, T., Takahashi, T., Ogawa, H., Irikura, K.,
794 Thio, H. K., Somerville, P. G., Fukushima, Y. and Fukushima, Y. (2006). Attenuation relations
795 of strong ground motion in Japan using site classification based on predominant period.
796 *Bulletin of the Seismological Society of America*, Vol. 96, No. 3, pp. 898-913.

797

798

799 Manuela Villani, Ove Arup & Partners Int'l Ltd, London, UK, manuela.villani@arup.com

800 Barbara Polidoro, Ove Arup & Partners Int'l Ltd, London, UK, barbara.polidoro@arup.com

801 Thomas Ader, Ove Arup & Partners Int'l Ltd, London, UK, thomas.ader@arup.com

802 Rory McCully, Ove Arup & Partners Int'l Ltd, London, UK, rory.mccully@arup.com

803 Ziggy Lubkowski, Ove Arup & Partners Int'l Ltd, London, UK, ziggy.lubkowski@arup.com

804 Tim J. Courtney, Horizon Nuclear Power, Gloucester, UK,

Tim.Courtney@Horizonnuclearpower.com

806 Martin Walsh, Horizon Nuclear Power, Gloucester, UK,

Martin.Walsh@Horizonnuclearpower.com

808

809

TABLES

810 Table 1 – Coefficients of the Rietbrock and Edwards (2017) GMPE for the UK.

T (s)	C ₁	C ₂	C ₃	C ₄	C ₅	C ₆	C ₇	C ₈	C ₉	C ₁₀	C ₁₁	σ_T	σ_B	σ_W
PGV	-4.596	1.699	-0.108	-1.609	0.198	-1.626	0.154	-2.317	0.067	-0.001	2.389	0.274	0.224	0.157
0.00	-2.334	1.695	-0.130	-1.848	0.215	-1.830	0.162	-1.970	0.068	-0.002	2.076	0.337	0.292	0.169
0.03	-1.518	1.610	-0.127	-2.198	0.240	-2.114	0.181	-1.712	0.089	-0.003	1.498	0.369	0.301	0.213
0.05	-1.830	1.649	-0.124	-1.744	0.174	-1.683	0.127	-1.530	0.070	-0.003	1.425	0.356	0.304	0.185
0.10	-2.481	1.777	-0.131	-1.437	0.142	-1.404	0.098	-1.786	0.039	-0.002	1.719	0.330	0.294	0.150
0.20	-3.575	2.040	-0.149	-1.283	0.130	-1.251	0.084	-2.028	0.027	-0.001	1.938	0.305	0.269	0.143
0.25	-4.049	2.155	-0.157	-1.241	0.125	-1.208	0.080	-2.081	0.024	-0.001	1.921	0.297	0.259	0.146
0.50	-5.643	2.502	-0.178	-1.112	0.106	-1.088	0.067	-2.173	0.017	-0.001	1.674	0.278	0.226	0.161
1.00	-6.845	2.624	-0.175	-1.030	0.096	-1.049	0.066	-2.205	0.012	0.000	1.579	0.265	0.197	0.177
2.00	-6.993	2.357	-0.139	-1.150	0.122	-1.230	0.099	-2.239	0.017	0.000	1.809	0.256	0.173	0.190
4.00	-6.514	1.913	-0.094	-1.441	0.171	-1.525	0.147	-2.355	0.050	0.000	2.037	0.245	0.145	0.198
5.00	-6.412	1.795	-0.082	-1.512	0.182	-1.588	0.157	-2.426	0.067	0.000	2.046	0.242	0.136	0.200

811

812

813

814

815

816

817

818 Table 2 – Main features of the recorded earthquakes in the UK.

Earthquake Name	Date	Lat. (°)	Long. (°)	Depth (km)	M _L	M _w	Number of Records	R _{epi} Range (km)	PGA Range Geometric Mean (cm/s ²)
Penzance	10/11/1996	50.00	-5.58	8.3	3.8	3.2 _l	1	34	3.59
Arran	04/03/1999	55.40	-5.24	19	4.0	3.2 _l	1	135	0.43
Sennybridge	25/10/1999	51.97	-3.57	14.1	3.6	3.3 _l	1	38	2.57
Warwick	23/09/2000	52.28	-1.61	14.4	4.2	3.3 _l	3	76 to 101	0.51 to 1.94

Melton Mowbray	28/10/2001	52.84	-0.85	14.4	4.1	3.4 ₁	2	16 to 143	0.99 to 18.26
Dudley	22/09/2002	52.53	-2.16	14	4.7	4.2 ₁	9	80 to 383	0.05 to 9.79
Folkestone	28/04/2007	51.10	1.17	5.3	4.3	4.0 _{2,3}	11	2 to 396	0.02 to 100
Market Rasen	27/02/2008	53.40	-0.33	17.8	5.2	4.5 _{3,7}	18	93 to 412	0.11 to 9.99
Lley Peninsula	29/05/2013	52.88	-4.72	10.5	3.8	3.7	7	50 to 175	0.17 to 2.29
Bristol Channel	20/02/2014	51.36	-4.16	3.5	4.1	3.7 _{4,7}	12	47 to 281	0.04 to 0.54
Ramsgate	22/05/2015	51.30	1.44	12.1	4.2	3.8 ₇	6	27 to 280	0.11 to 1.63
Swansea	17/02/2018	51.77	-3.83	7.0	4.6	4.3 ₈	12	63 to 187	0.24 to 8.23
1: Sargeant and Ottermöller (2009); 2: Ottermöller et al. (2009); 3: Ottermöller and Sargeant (2010); 4: Hicks (2014a); 5: Hicks(2014b); 6: Hicks (2015); 7: Rietbrock and Edwards (2017); 8: From correlation between M _L and M _w from Akkar et al. (2009)									

819

820

821

822

823

824

825

826 Table 3 – Site Classification of the recording stations.

Station ID	Lat (°)	Long (°)	Site Description (Provided by the BGS or Based on Geological Maps)		V _{s30} Based on Geological Description (#) (m/s)	Site Classification Based on H/V Ratio (°)	Assumed V _{s30} (m/s)
			Rock Outcrop / Underlying Rock Type	Seismometer Foundation			
AEU	52.620	1.235	Cretaceous Chalk	Sand/gravel drift deposits and topsoil (< 15m thick)	375 to 700	Very hard rock	500(*)

APA	52.300	1.478	Crag Group	Lowestoft Formation – Chalky Till with outwash Sands and Gravels, Silts and Clays	200 to 375	Soft stiff soil	300 (+)
BCC	55.015	-3.220	Sherwood Sandstone	Shallow soil	540 to 1,050	N/A	760 (*)
CCA1	50.186	-5.228	Saprolite (Weathered Granite)	Bedrock	700 to 1,400	Hard rock	845 (Tallet-Williams and Fenton, 2015)
CRQ	50.167	-5.173	Carmenellis Intrusion – Granite	Bedrock	700 to 1,400	N/A	760 (*)
CWF	52.738	-1.307	Neoproterozoic Volcaniclastic Breccia	Topsoil (1-2m)	700 to 1,400	Hard rock	1,050 (+)
DYA	50.435	-3.931	Granite Batholith	Saprolite (in-situ rock weathering products, <1m thick)	700 to 1,400	Hard rock	1,050 (+)
EDI	55.923	-3.186	Andesite	Isolated Concrete Pier on Bedrock	700 to 1,400	Hard rock	1,500 (-)
ELSH	51.148	1.137	Middle Cretaceous Chalk	Weathered Chalk	375 to 700	Soft soil	200 (-)
ESK	55.317	-3.205	Silurian Greywacke	Isolated Concrete Pier on Bedrock	1,050 to 1,400	Very hard rock	2,000 (-)
FOEL	52.890	-3.201	Llangynog Formation – Sandstone and Mudstone	Bedrock	540 to 1,050	Rock	760 (+)
GAL1	54.866	-4.711	Silurian Greywacke	Bedrock	700 to 1,400	Very hard rock	2,000 (-)
HBL2	52.051	-3.038	Saltwick Formation – Sandstone, Siltstone and Mudstone	Shallow soil	540 to 1,050	N/A	760 (*)
HLM1	52.518	-2.881	St Maughans Formation - Argillaceous Rocks and Sandstone	Head (rock fragments/soil creep deposit, 1 to 2m thick)	540 to 1,050	Hard rock	1,000 (+)

HPK	53.955	-1.624	Neoproterozoic Sandstone	Glacial Till drift deposit (> 3m thick)	540 to 1,050	Rock	760 (+)
HTL	50.994	-4.485	Carboniferous Sandstone	Weathered bedrock	540 to 1,050	Hard rock	1,000 (+)
JSA	49.188	-2.171	Carboniferous Sandstone	Unknown	N/A	Hard rock	1500 (-)
KEY2	52.877	-1.075	Unknown	Lias	375 to 700	N/A	550(*)
LBWR	53.402	-1.725	Blue Anchor Formation – Mudstone	Shale Grit	540 to 1,050	Rock	760 (+)
LDU	53.803	-1.555	Carboniferous Sandstones/Shales	Bedrock	540 to 1,050	Hard rock	1,000 (+)
LDU2	53.803	-1.555	Pennine Lower Coal Measures Formation – Sandstone, Siltstone and Mudstone	Bedrock	540 to 1,050	Hard rock	1,000 (+)
LMK	53.457	-0.327	Pennine Lower Coal Measures Formation – Sandstone, Siltstone and Mudstone	Bedrock	540 to 1,050	Stiff soil	550 (+)
MCH	51.998	-2.998	Carstone Formation – Sandstone	Bedrock	540 to 1,050	Rock	760 (+)
MCH1	51.998	-2.998	Devonian-Silurian, interbedded Sandstones/Siltstones	Bedrock	540 to 1,050	Rock	760 (+)
MON M	51.839	-2.804	Old Red Sandstone	Devonian sandstones/siltstones (interbedded)	540 to 1,050	N/A	760 (*)
OLDB	51.661	-2.551	Mercia Mudstone	Tidal Flats	100 to 375	Soft soil	180 (+)
PGB1	55.810	-4.478	Vesicular Basalt	Heavily weathered porous bedrock	> 760	Rock	760 (-)
RSBS	51.953	-4.745		Mudstone shale formation/igneous intrusion	1,500 to 2,300(**)	N/A	2000 (*)
SPK1	54.434	-3.488	Chalk	Bedrock	375 to 700	N/A	500 (*)
STNC	53.091	-2.206	Carboniferous Sandstone/Siltstone/Mudstone	Glacial Till/Topsoil (> 3m thick)	540 to 1,050	Rock	760 (*)

STRD	51.776	-2.164	Birdlip Limestone Formation	Bedrock	540 to 1,050	Stiff soil / Rock	600 (*)
SWN	51.513	-1.801	Cretaceous Chalk	Topsoil (< 1m thick)	375 to 700	Stiff soil	503 (+)
SWN1	51.513	-1.800	Cretaceous Chalk	Bedrock	375 to 700	Stiff soil	503 (Tallet-Williams and Fenton, 2015)
TFO1	51.114	1.141	Cretaceous Chalk	Sandy Clay with Flints	375 to 700	Stiff soil	480 (+)
WACR	52.725	0.627	Chalk	Lowestoft Formation – Chalky Till with outwash sands and gravels, silts and clays. (2-18m thick)	100 to 300	Soft soil	200 (+)
WLF1	53.289	-4.397	Hornfel Lens in Granite Terrane	Bedrock	700 to 1,400	Very hard rock	2500 (-)
WOL	51.313	-1.223	Chalk	Bedrock	375 to 700	Unclear	500 (*)
WPS	53.400	-4.499	New Harbour Group	Glacial Till (very thin)	2,300 to 3,000	Very hard rock	2,000 (+)

Note:

(*) Geology preferred, (-) = H/V preferred, (+) = Geology and H/V ratio broadly correlate

(#) Ranges based on Borchedt (1994) for all stations except PGB1 station which is based on Christensen et al. (1980), see Section 2.1.

(°) Based on Di Alessandro et al. (2012).

(**) Based on Press (1966).

(+) Estimated surface V_{s30} from data at adjacent Wylfa Development Area

827

828

829

830

831

832

833

Table 4 – Main features of the UK earthquakes in the macroseismic database.

Event	Date	Lat (°)	Long (°)	M _L	M _w	Max Intensity	Number of IDPs
Dover Straits	06/04/1580	51.06	1.60	5.8	5.5	7-8	91
Swansea	08/09/1775	51.73	-3.81	5.1	4.8	7	74
Whitehaven	11/08/1786	54.53	-3.68	5.0	4.7	6-7	57
Inverness	13/08/1816	57.43	-4.33	5.1	4.8	7-8	72
Lancaster	20/08/1835	54.02	-2.69	4.4	4.1	5-6	70
Lancashire	17/03/1843	54.00	-3.60	5.1	4.8	5	117

Event	Date	Lat (°)	Long (°)	M _L	M _w	Max Intensity	Number of IDPs
Caernarvon	09/11/1852	53.05	-4.43	5.3	5.0	7	222
Newquay	13/01/1860	50.46	-5.31	4.0	3.7	5-6	71
Hereford	06/10/1863	52.00	-2.80	5.2	4.9	6	298
Neath	30/10/1868	51.73	-3.67	4.9	4.6	5-6	186
Appleby	17/03/1871	54.71	-2.47	4.9	4.6	6	334
Colchester	22/04/1884	51.82	0.90	4.6	4.3	8	414
Invergarry	02/02/1888	57.10	-5.14	4.8	4.5	5-6	133
Edinburgh	18/01/1889	55.87	-3.36	3.2	3.0	5	64
Inverness	15/11/1890	57.46	-4.35	4.5	4.2	6	141
Pembroke	18/08/1892	51.70	-5.04	5.1	4.8	7	179
Leicester	04/08/1893	52.72	-1.22	3.7	3.4	7	130
Carmarthen	02/11/1893	51.81	-4.41	5.0	4.7	7	131
Hereford	17/12/1896	52.02	-2.55	5.3	5.0	7	735
Carlisle	09/07/1901	54.80	-3.04	4.1	3.8	6	64
Inverness	18/09/1901	57.43	-4.32	5.0	4.7	7	172
Derby	24/03/1903	53.05	-1.70	4.6	4.3	7	176
Caernarvon	19/06/1903	53.03	-4.28	4.9	4.6	6	80
Derby	03/07/1904	53.05	-1.75	4.2	3.9	6	220
Doncaster	23/04/1905	53.40	-0.99	4.3	4.0	5-6	203
Swansea	27/06/1906	51.62	-3.81	5.2	4.9	7	310
Derby	27/08/1906	53.09	-1.51	3.5	3.3	5	52
Stafford	14/01/1916	52.85	-2.19	4.6	4.3	7	143
South Brent	25/12/1923	50.47	-3.86	3.3	3.1	5	82
Ludlow	15/08/1926	52.31	-2.66	4.8	4.5	7	300
Dogger Bank	07/06/1931	54.08	1.50	6.1	5.8	7	887
Wensleydale	14/01/1933	54.30	-2.15	4.4	4.1	6-7	109
Torridon	16/08/1934	57.54	-5.34	4.1	3.8	6	71
Caernarvon	12/12/1940	53.03	-4.18	4.7	4.4	5	100
Skipton	30/12/1944	53.86	-2.02	4.8	4.5	7	115
Ashby	10/01/1956	52.72	-1.27	3.6	3.3	6	64
Derby	12/02/1957	52.82	-1.33	4.2	3.9	6	96
Chichester	25/10/1963	50.77	-0.97	4.7	4.4	5-6	53
Kirkby Stephen	09/08/1970	54.50	-2.47	4.1	3.8	5	69
Todmorden	07/03/1972	53.70	-2.03	4.0	3.7	6	84

Event	Date	Lat (°)	Long (°)	M _L	M _w	Max Intensity	Number of IDPs
Bala	23/01/1974	52.98	-3.49	3.5	3.3	5	111
Newport	25/02/1974	51.64	-3.05	3.9	3.6	5	192
Carlisle	26/12/1979	55.03	-2.82	4.7	4.4	6	652
Carlisle	01/01/1980	55.03	-2.79	3.8	3.5	5	61
Felindre	15/04/1984	52.41	-3.25	3.3	3.1	4	63
Lleyn Peninsula	19/07/1984	52.96	-4.38	5.4	5.1	7	342
Oban	29/09/1986	56.45	-5.65	4.1	3.8	5	76
Bishop's Castle	02/04/1990	52.43	-3.03	5.1	4.8	6	2,350
Peterborough	17/02/1992	52.49	-0.20	3.4	3.2	5	144
Caernarvon	29/07/1992	53.13	-4.39	3.5	3.3	5	115
Norwich	15/02/1994	52.56	0.91	4.0	3.7	5	302
Shrewsbury	07/03/1996	52.80	-2.74	3.4	3.2	5	63
Penzance	10/11/1996	50.00	-5.58	3.8	3.2	5	96
Arran	04/03/1999	55.40	-5.24	4.0	3.2	5	228
Caernarvon	01/09/1999	53.19	-4.34	3.2	3.0	4	37
Sennybridge	25/10/1999	51.96	-3.57	3.6	3.3	5	112
Warwick	23/09/2000	52.28	-1.61	4.2	3.3	5	282
Bude	31/05/2001	51.01	-4.63	3.6	3.3	5	118
Folkestone	28/04/2007	51.10	1.17	4.3	4.0	6	50
Market Rasen	27/02/2008	53.40	-0.33	5.2	4.5	6	641
Masham	03/01/2011	54.17	-1.70	3.6	3.3	4	166
Ashwell	28/01/2015	52.73	-0.72	3.8	3.5	5	106
Broadstairs	22/05/2015	51.30	1.44	4.2	3.9	5	109

834

835

836

837

838

839

Table 5 – Summary of GMPE Database and Range of Applicability

GMPE	Magnitude Range (M _w)	Distance Range (km)	Period Range (s)	Distance Metric	Definition of Ground Motion	VS30 range (m/s)	Max PGA(g) in Database
Abrahamson et al. (2014), ASK14	3.0 to 8.5	0 to 300	PGA, 0.01-10 s	Rrup	RotD050	180 to 1,000	1.77
Boore et al. (2014), BSSA14	3.0 to 8.5	0 to 400	PGA, 0.01-10 s	Rjb	RotD050	150 to 1,500	1.77

Campbell and Bozorgnia (2014), CB14	3.3 to 8.5	0 to 300	PGA, 0.01-10 s	Rrup	RotD050	150 to 1,500	1.77
Chiou and Youngs (2014), CY14	3.5 to 8.5	0 to 300	PGA, 0.01-10 s	Rrup	RotD050	150 to 1,500	1.77
Akkar et al. (2014), ASB14	4.0 to 7.6	0 to 200	PGA, 0.01-4 s	Repi, Rhyp or Rjb	GM	150 to 1,200	0.99
Bindi et al. (2014), BI14	4.0 to 7.6	0 to 300	PGA, 0.01-3 s	Rhyp or Rjb	GM	150 to 1,000	0.98
Cauzzi et al. (2015) CA15	4.5 to 7.9	0 to 150	0.01-10 s	Rrup	GM	150 to 1,500	1.6
Rietbrock and Edwards (2017), RE17	3.0 to 7.0	1 to 300	PGA, 0.033-5 s	Rjb	GM	Very hard Rock	Based on simulations
GM = Geometric mean of two horizontal and orthogonal components							
RotD050 = The 50th percentile of the response spectra over all non-redundant rotation angles (Boore, 2010)							

840

841 Table 6 – Average κ_{host} values computed for the eight preselected GMPEs.

GMPE	κ_{host} (s) with $V_{S30}=550\text{m/s}$	κ_{host} (s) with $V_{S30}=760\text{m/s}$
ASK14	0.059	0.051
BSSA14	0.048	0.046
CB14	0.046	0.037
CY14	0.047	0.042
ASB14	0.044	0.041
BI14	0.043	0.042
CA15	0.041	0.038

842 Table 7 – Summary of the Performance of the GMPEs with Respect to the Residuals

GMPE	Magnitude Trends	Distance Trends	Residual Range	Mean Residuals for Distance < 100 km
ASK14	No trend	No strong trend	-2.7 to 3.4	0 to 1
BSSA14	No trend	No strong trend	-2.5 to 3.5	0.3 to 1.7
CB14	No strong Trend	Linear trend	-2.1 to 3.2	0.3 to 1.3
CY14	No trend	Linear trend	-2.6 to 3.3	0.1 to 1.7
ASB14	Linear trend	No strong trend	-2.7 to 3.2	-0.5 to 1.6
BI14	No trend	No trend	-0.9 to 3.6	0.5 to 1.6
CA15	No strong trend	No strong trend	-2.5 to 3.2	-0.5 to 1.4
RE17	No trend	No trend	-3.6 to 3.5	-0.3 to 1.4

843 Table 8 –Performance results with respect to the UK ground motion dataset.

GMPE	Scherbaum et al. (2009)	Kale and Akkar (2013)		
	LLH	MDE	k _{0.5}	EDR
<u>ASK14</u>	<u>2.67</u>	<u>1.30</u>	<u>1.22</u>	<u>1.59</u>
BSSA14	3.16	1.49	1.31	1.97
CB14	3.49	1.56	1.31	2.06
CY14	3.40	1.50	1.30	1.96
BI14	3.02	1.44	1.35	1.95
<u>CA15</u>	<u>2.78</u>	1.38	1.25	1.73
<u>RE17</u>	<u>2.42</u>	<u>1.09</u>	<u>1.12</u>	<u>1.21</u>

Note: Underlined values represent best three values for each of the GMPEs assessed.

844 Table 9 – Intensity Correlations Considered Against the UK Data

Intensity Correlation	Data from	Intensity range
Atkinson and Kaka (2007)	California and Central US	I – IX
Faenza and Michelini (2009)	Italy	II – VIII
Tselentis and Danciu (2008)	Greece	IV – VIII
Wald et al. (1999)	California	V – VIII
Faccioli and Cauzzi (2006)	Italy	V – IX
Worden et al. (2012)	California	II – IX

845 Table 10 – Performance of Preselected GMPEs Against the UK Macroseismic Data

GMPE	Faccioli and Cauzzi (2006)				Atkinson and Kaka (2007)			
	Scherbaum et al. (2009)	Kale and Akkar (2013)			Scherbaum et al. (2009)	Kale and Akkar (2013)		
	LLH	EDR	k _{0.5}	MDE	LLH	EDR	k _{0.5}	MDE
ASB14	2.39	1.42	1.11	1.57	2.33	1.39	1.28	1.79
ASK14	2.13	<u>1.31</u>	<u>1.00</u>	<u>1.31</u>	2.00	1.26	<u>1.06</u>	<u>1.34</u>
BI14	2.44	1.33	1.16	1.55	2.37	1.37	1.38	1.88
BSSA14	2.30	1.39	1.08	1.50	2.25	1.37	1.21	1.66
CA15	2.19	<u>1.23</u>	<u>1.07</u>	<u>1.32</u>	2.15	1.26	1.27	<u>1.60</u>
CY14	2.16	1.31	<u>1.01</u>	<u>1.32</u>	2.06	1.27	1.10	1.40
CB14	2.56	1.53	1.17	1.80	2.50	1.49	1.37	2.04
RE17	2.15	<u>1.22</u>	1.12	1.36	2.19	1.29	1.34	1.73

Note: Underlined values represent best three values for each of the method adopted.

846

847

848

849

850

851

852

853

854

855

LIST OF FIGURES CAPTIONS

856 Figure 1. κ_0 values at the UK ground motion stations (grey circles) according to Rietbrock and
857 Edwards (2017). Squares represent the average values in soil classes and their uncertainty.

858 Figure 2. Comparison between the spectral acceleration at $T=0$ s (PGA) Rietbrock et al. (2013)
859 and Rietbrock and Edwards (2017).

860 Figure 3. Comparison of the QLG attenuation for the UK (Ottomöler and Sargeant, 2009) and the
861 attenuation from other countries.

862 Figure 4. Geographical distribution of the earthquakes recorded in the UK.

863 Figure 5. Distribution of ground motion data in terms of magnitude versus (a) epicentral
864 distance, (b) VS30 and (c) PGA.

865 Figure 6. Geographical distribution of the macroseismic data.

866 Figure 7. Macroseismic dataset: intensity versus distance distribution for the (a) initial dataset
867 and (b) final dataset used in the analysis.

868 Figure 8. Examples of VS- κ_0 adjustment factors for soil, rock and hard rock for three GMPEs.

869 Figure 9. Comparison between ground motion data from four UK earthquakes and predictions
870 from the NGA West2 GMPEs

871 Figure 10. Comparison between ground motion data from four UK earthquakes (symbols) and
872 predictions from the GMPEs of Akkar et al. (2014), Bindi et al. (2014), Cauzzi et al. (2015) and
873 Rietbrock and Edwards (2017): black solid lines indicate the median predictions, while dashed
874 and dotted lines the 16th and 84th percentiles and the 5th and 95th percentiles respectively. The
875 median prediction from Rietbrock et al. (2013), RI13, is added to the plots for RE17.

876 Figure 11. Normalized model residuals between UK data and predictions from the NGA West2
877 GMPEs

878 Figure 12. Normalized model residuals between UK data and predictions from the GMPEs of
879 Akkar et al. (2014), Bindi et al. (2014), Cauzzi et al. (2015) and Rietbrock and Edwards (2017)

880 Figure 13. Results of the Scherbaum et al. (2009) test for the eight selected GMPEs

881 Figure 14. Results of the Kale and Akkar (2013) test for the eight selected GMPEs

882 Figure 15. Comparison of six correlations from literature between PGA and intensity (grey lines:
883 solid median prediction, dashed 5th -95th percentiles) against a subset of the UK data for which both
884 intensities and PGA were available (dots)

885 Figure 16. Examples of normalized model residuals between UK macroseismic data and
886 predictions from three GMPEs using the GMICE from Faccioli and Cauzzi (2006), FC06.

887 Figure 17. Comparisons among the response spectra predicted by the eight GMPEs at two
888 magnitude values ($MW=5$ and 6) and two epicentral distances ($R_{epi}=15$ and 50 km).

889 Figure 18. Similarities between GMPEs in terms of Euclidean distance (left) and Sammon's map
890 (right) for rock sites.

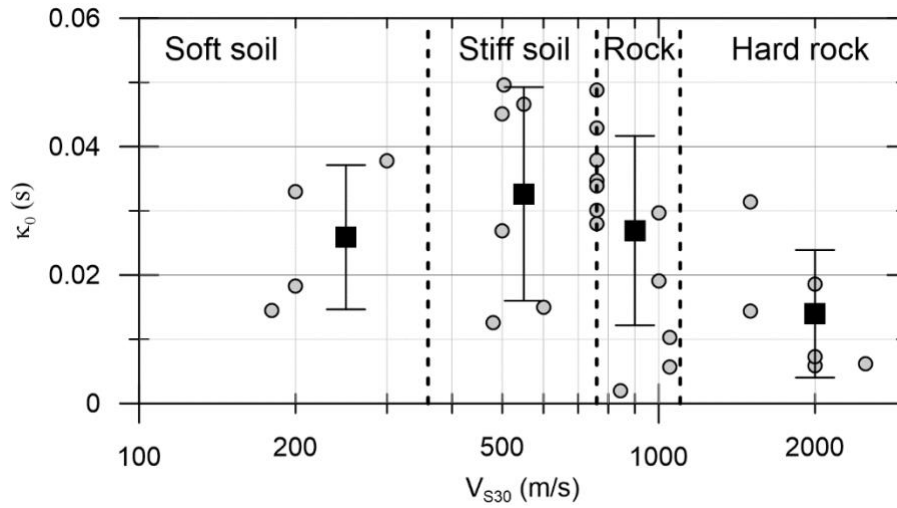
891 Figure 19. Similarities between GMPEs in terms of Euclidean distance (left) and Sammon's map
892 (right) for hard rock sites

893

894

895

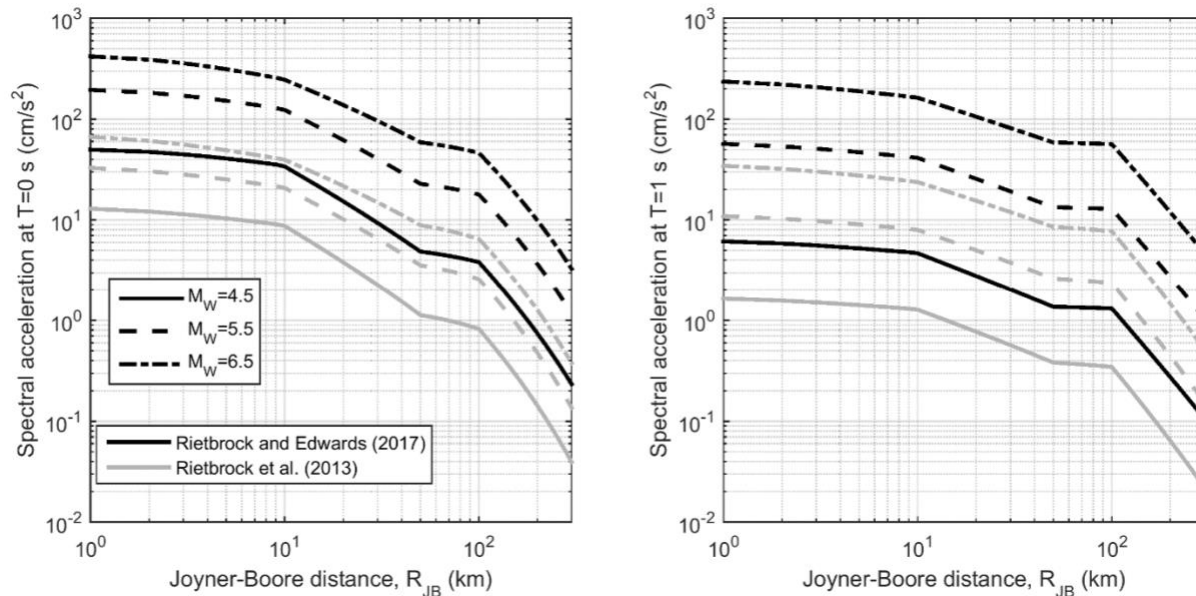
896 FIGURES



897

898 Figure 1. κ_0 values at the UK ground motion stations (grey circles) according to Rietbrock and Edwards

899 (2017). Squares represent the average values in soil classes and their uncertainty.

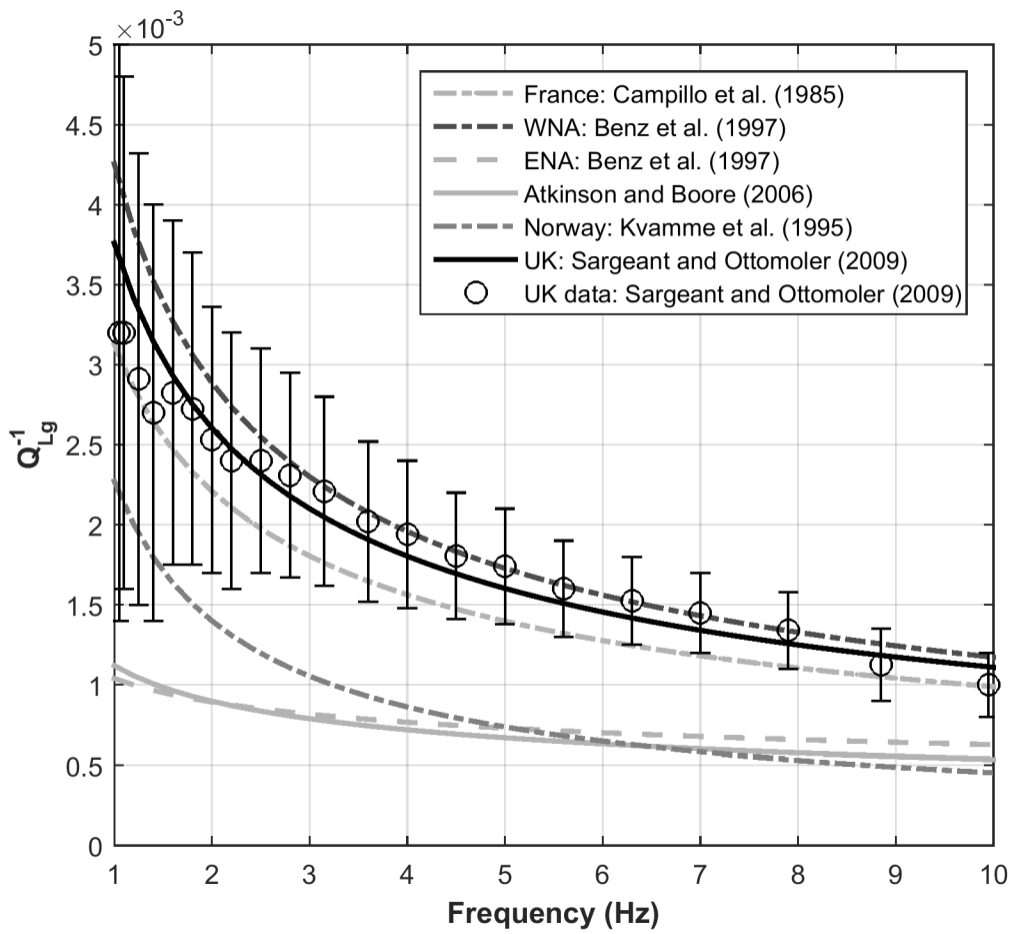


900

901 Figure 2. Comparison between the spectral acceleration at T=0 s (PGA) Rietbrock et al. (2013) and

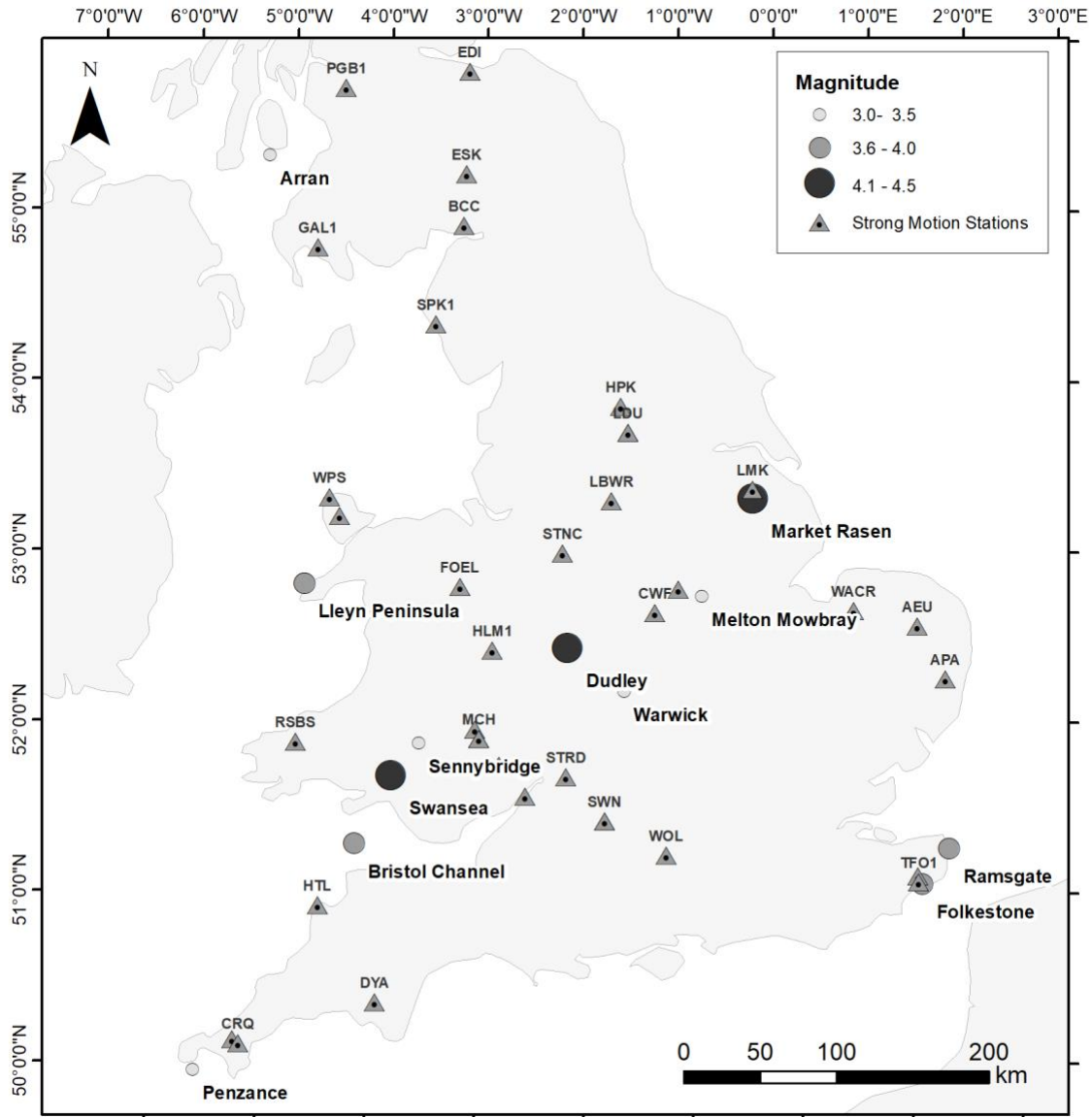
902 Rietbrock and Edwards (2017).

903



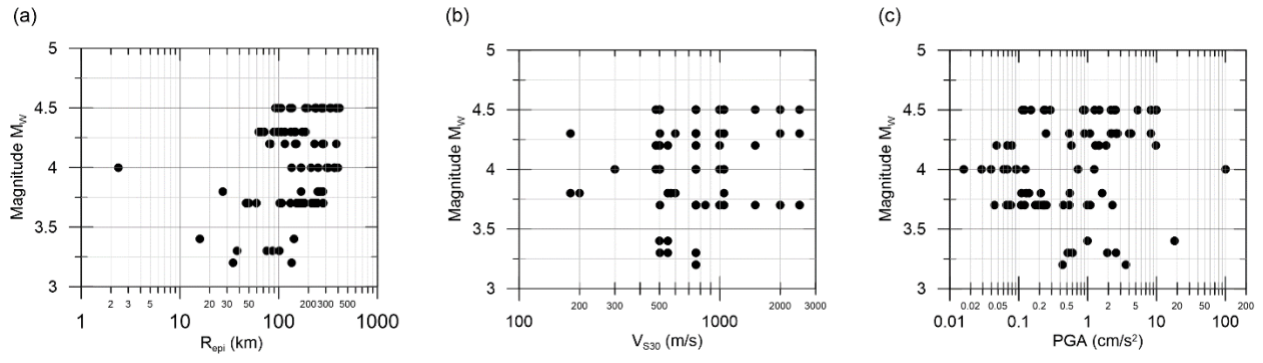
904 Figure 3. Comparison of the Q_{Lg} attenuation for the UK (Ottomoler and Sargeant, 2009) and the attenuation
 905 from other countries.
 906

907



908

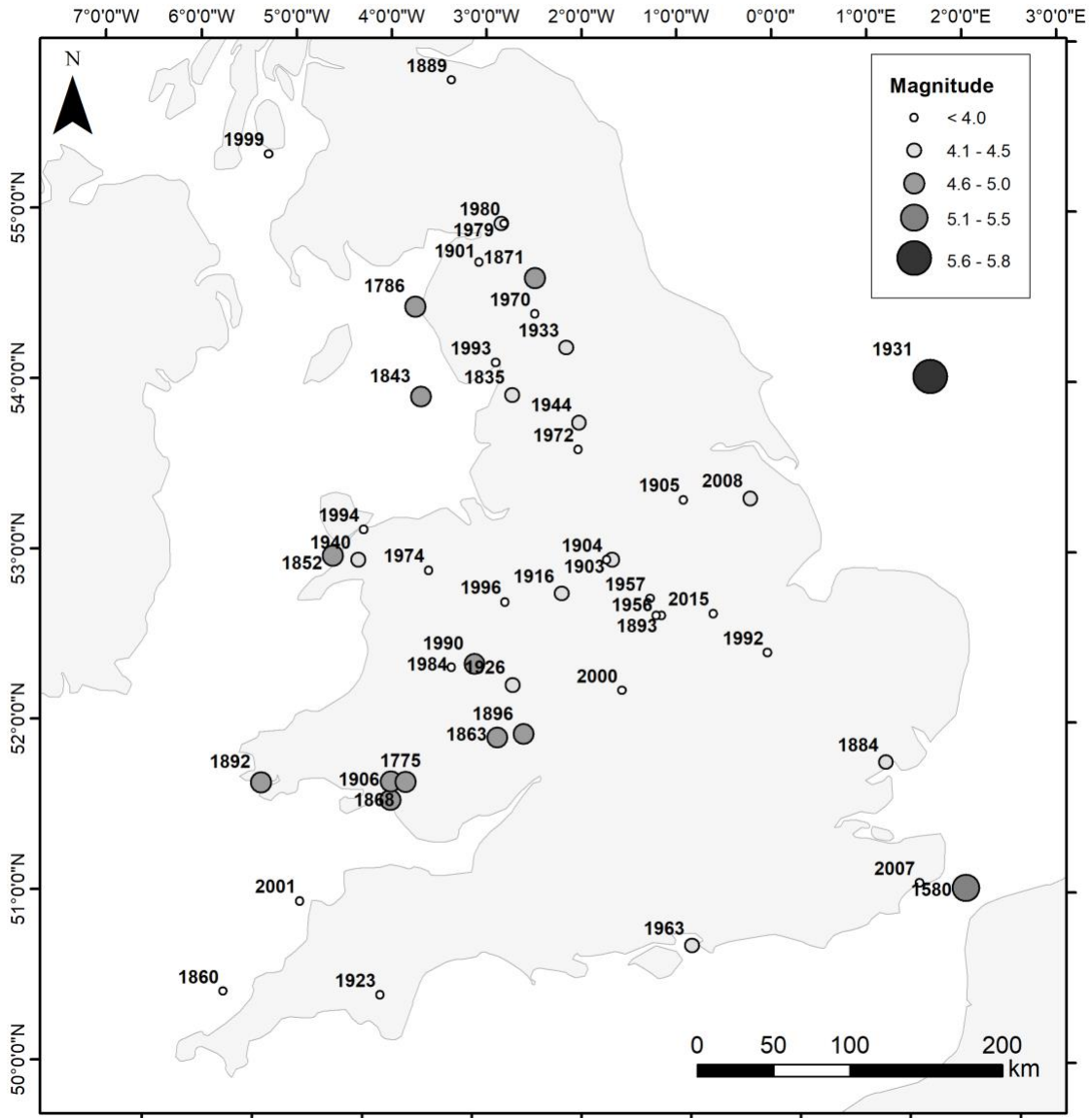
909 Figure 4. Geographical distribution of the earthquakes recorded in the UK.



910

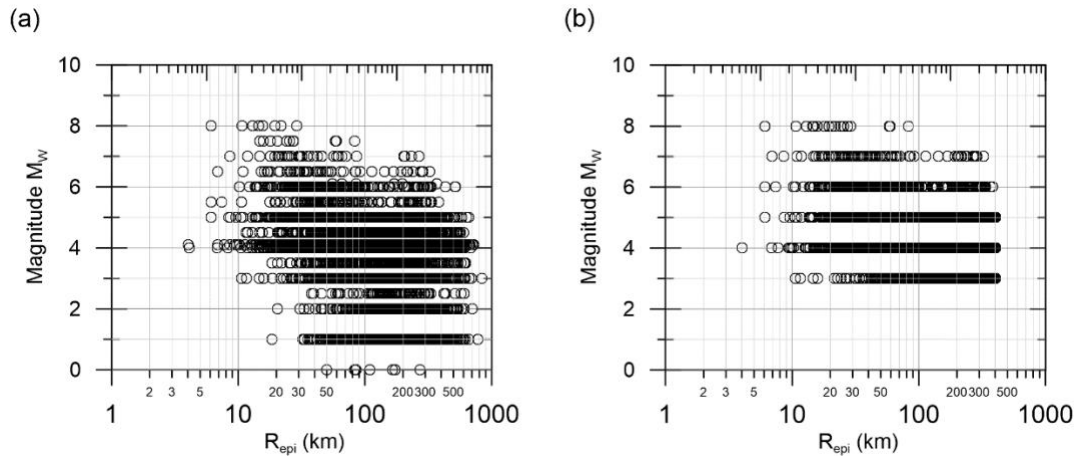
911 Figure 5. Distribution of ground motion data in terms of magnitude versus (a) epicentral distance, (b) V_{S30}

912 and (c) PGA.



913

914 Figure 6. Geographical distribution of the macroseismic data.



915

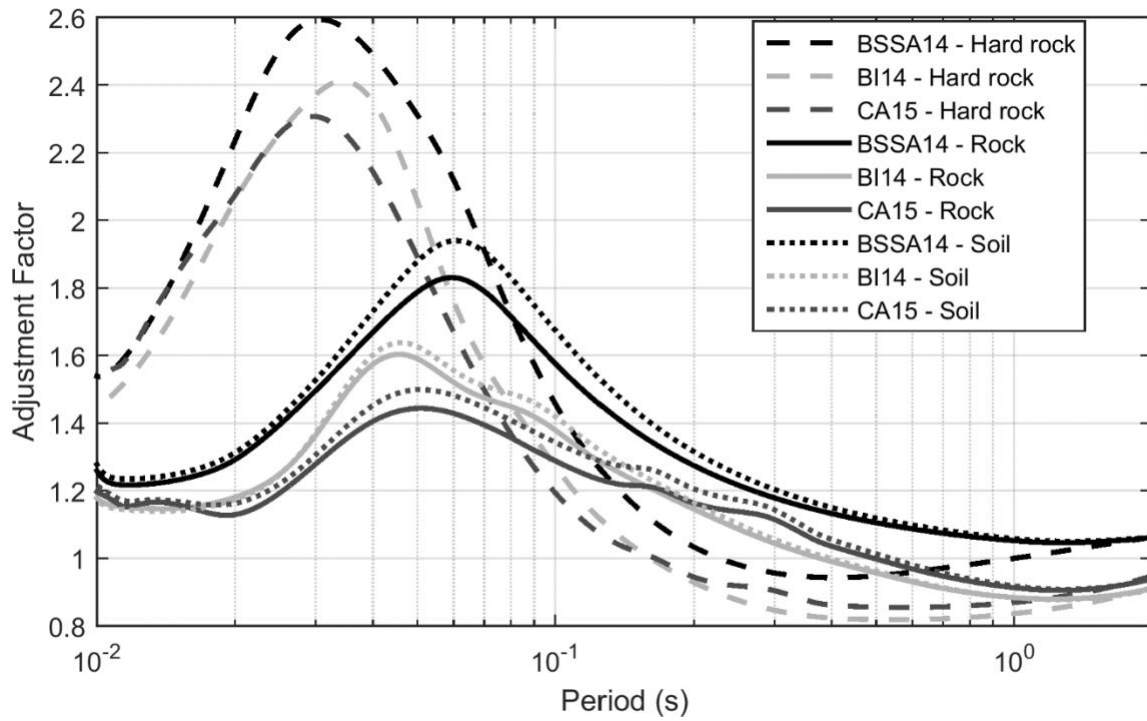
916 Figure 7. Macroseismic dataset: intensity versus distance distribution for the (a) initial dataset and (b) final

917 dataset used in the analysis.

918

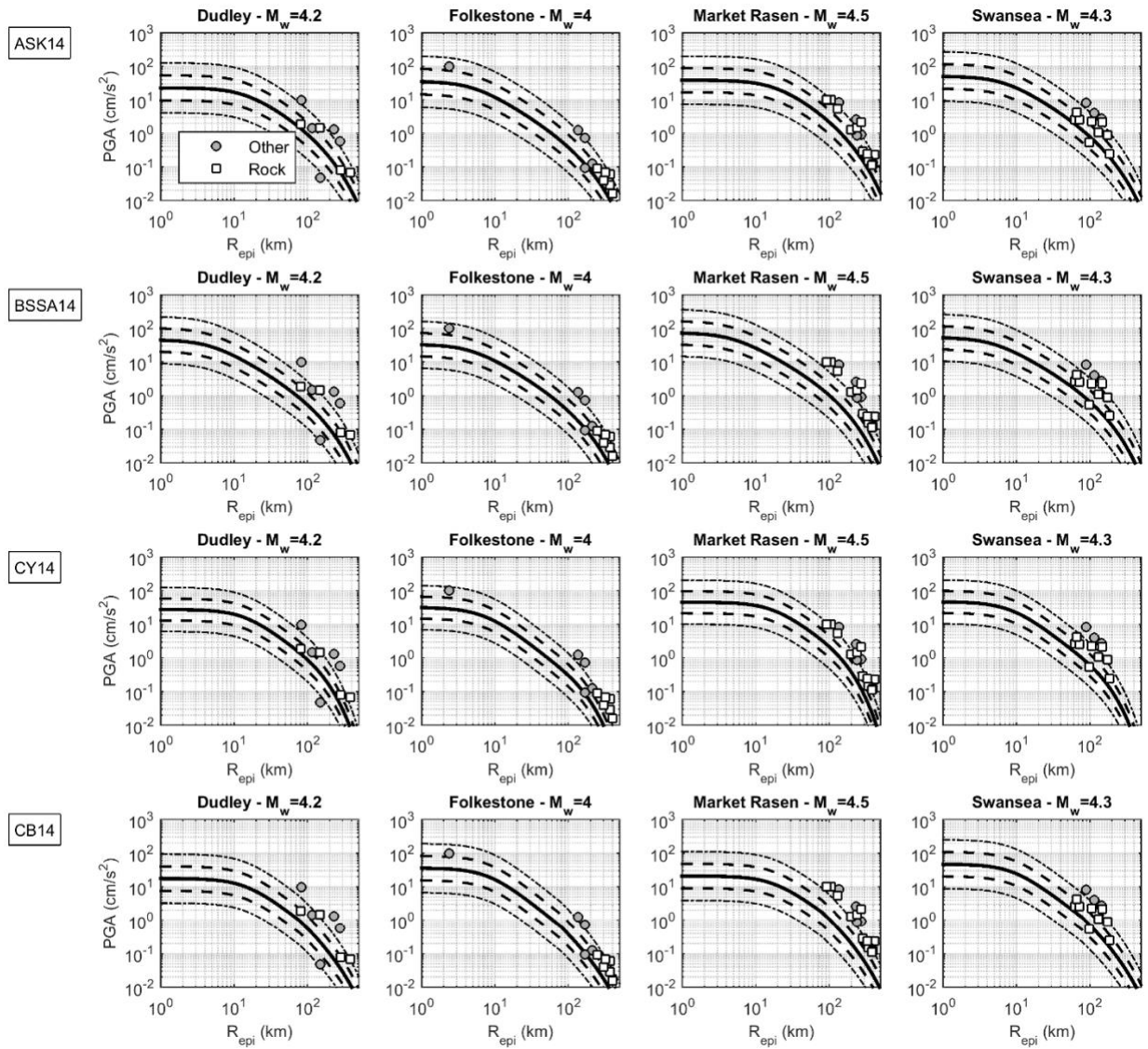
919

920



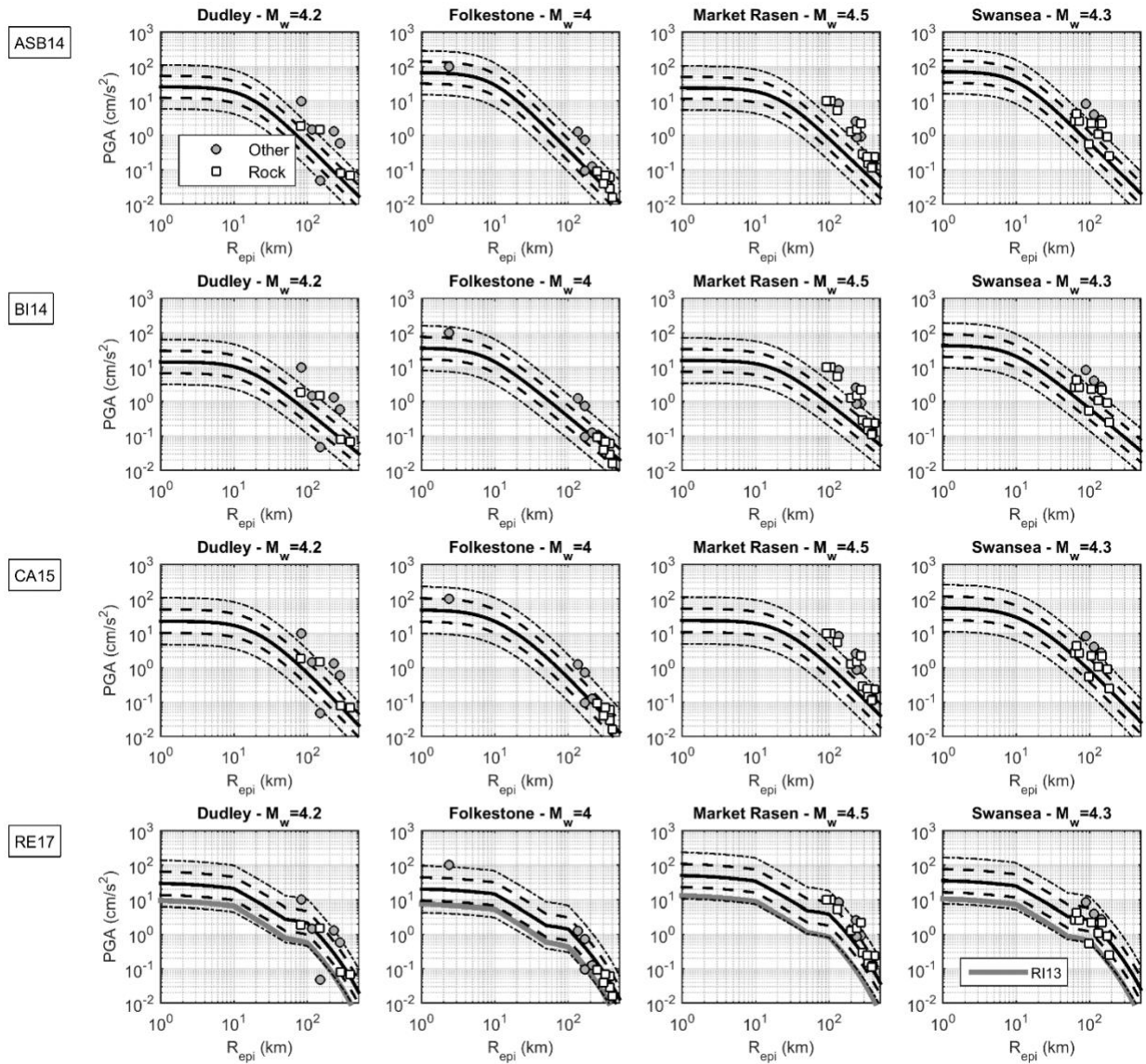
921

922 Figure 8. Examples of V_s - κ_0 adjustment factors for soil, rock and hard rock for three GMPEs.



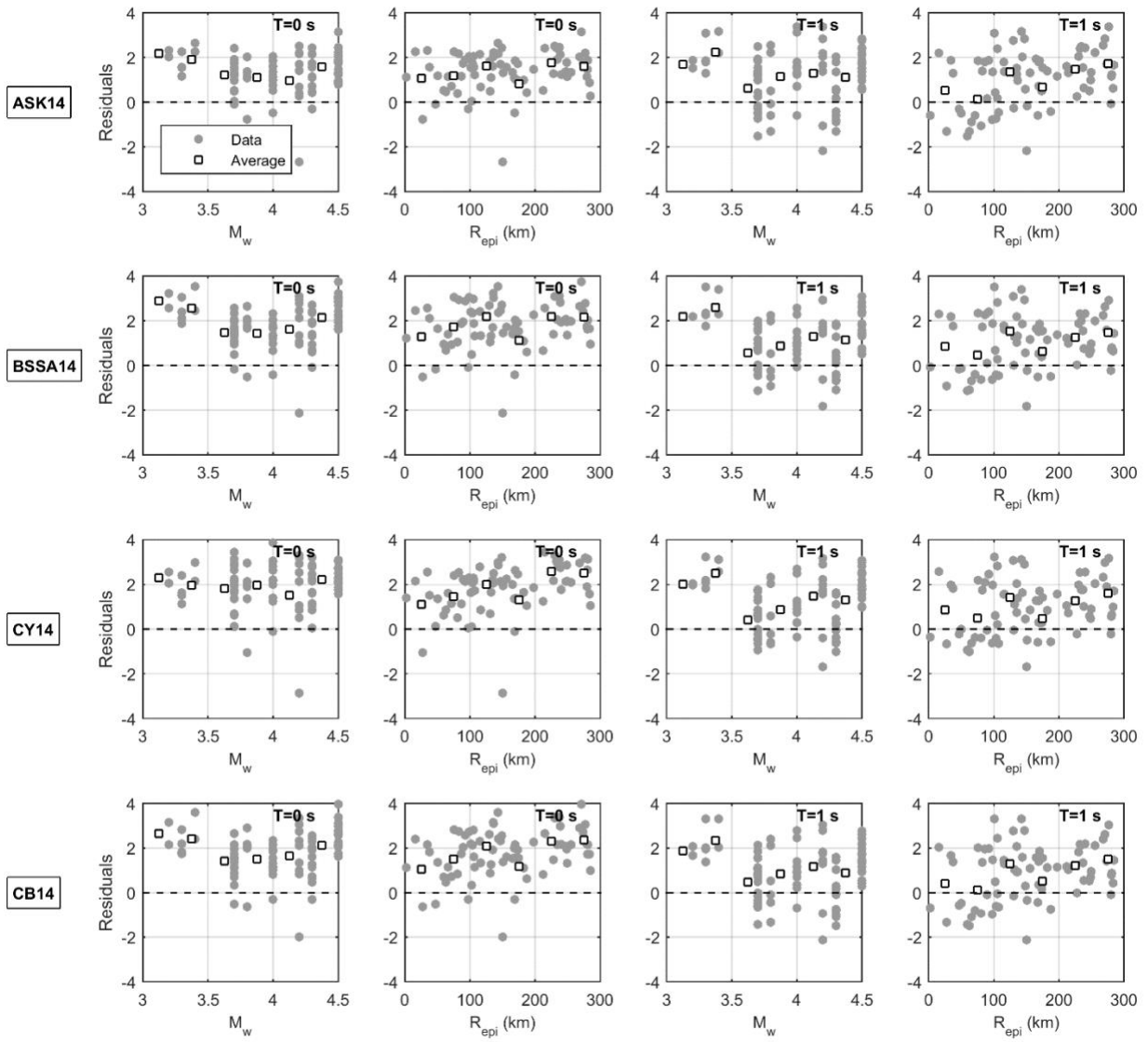
924

925 Figure 9. Comparison between ground motion data from four UK earthquakes and predictions from the
 926 NGA West2 GMPEs



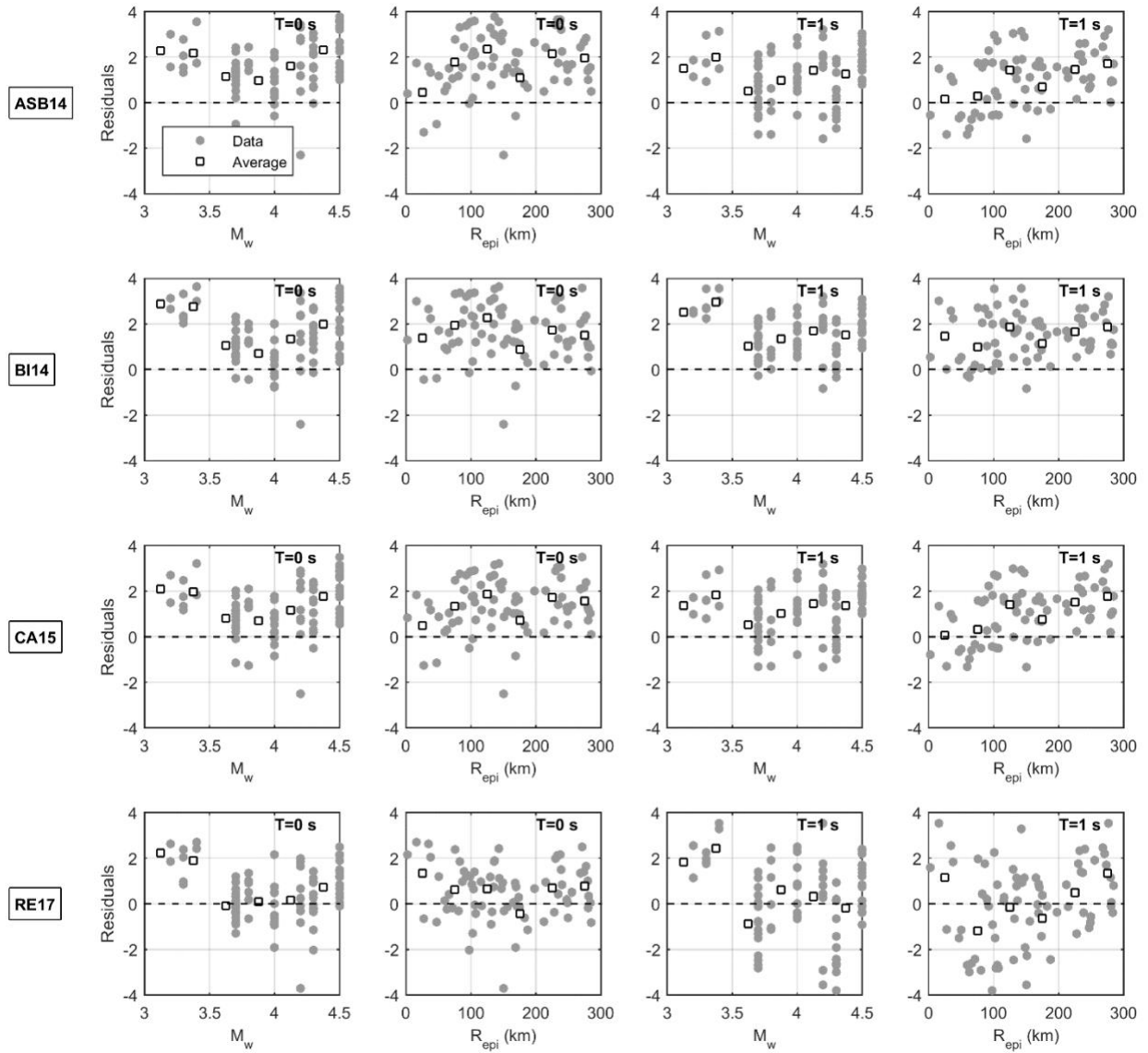
928

929 Figure 10. Comparison between ground motion data from four UK earthquakes (symbols) and predictions
 930 from the GMPEs of Akkar et al. (2014), Bindi et al. (2014), Cauzzi et al. (2015) and Rietbrock and Edwards
 931 (2017): black solid lines indicate the median predictions, while dashed and dotted lines the 16th and 84th
 932 percentiles and the 5th and 95th percentiles respectively. The median prediction from Rietbrock et al. (2013),
 933 RI13, is added to the plots for RE17.



934

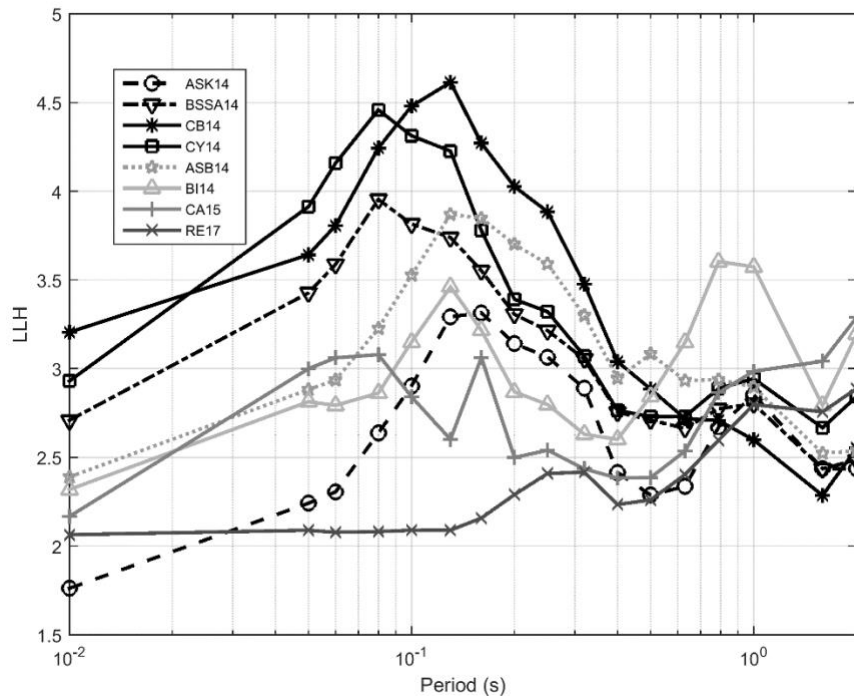
935 Figure 11. Normalized model residuals between UK data and predictions from the NGA West2 GMPEs



936

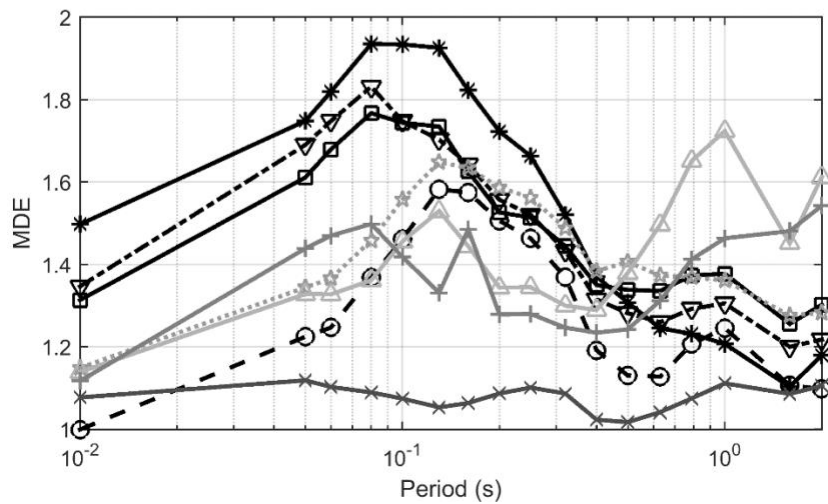
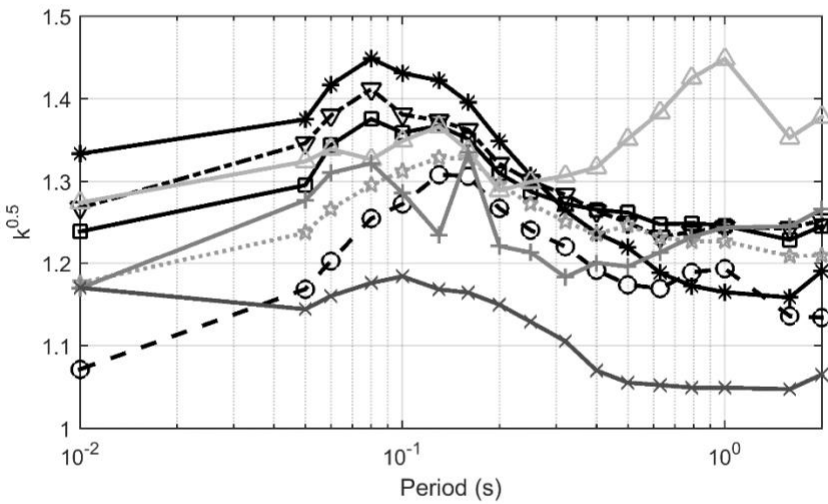
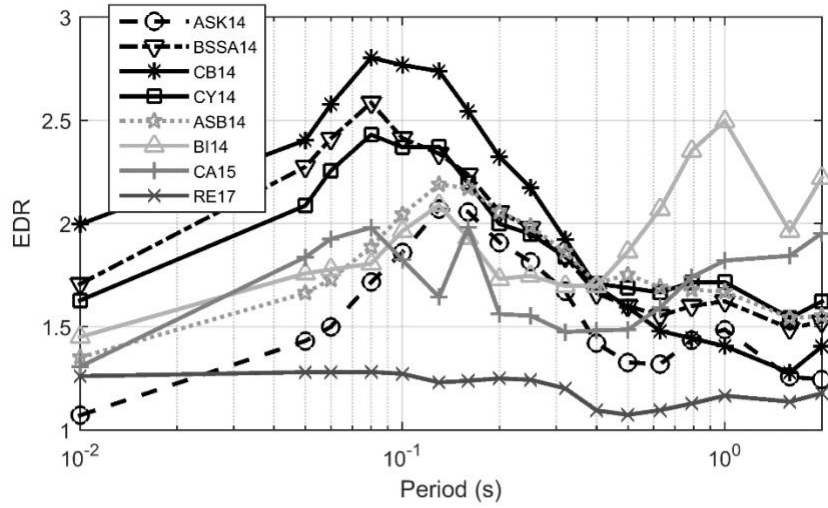
937 Figure 12. Normalized model residuals between UK data and predictions from the GMPEs of Akkar et al.

938 (2014), Bindi et al. (2014), Cauzzi et al. (2015) and Rietbrock and Edwards (2017)



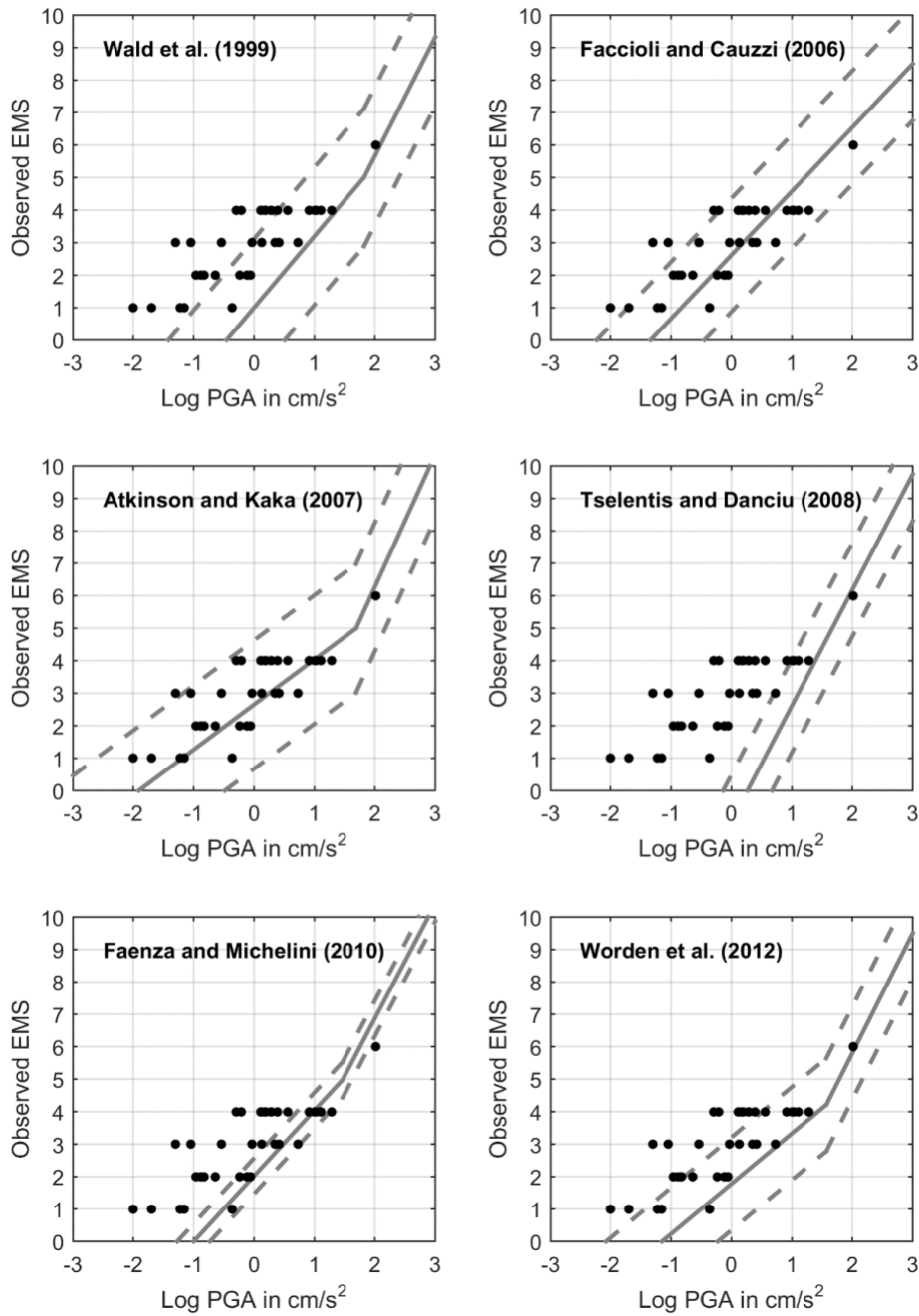
939

940 Figure 13. Results of the Scherbaum et al. (2009) test for the eight selected GMPEs



941

942 Figure 14. Results of the Kale and Akkar (2013) test for the eight selected GMPEs

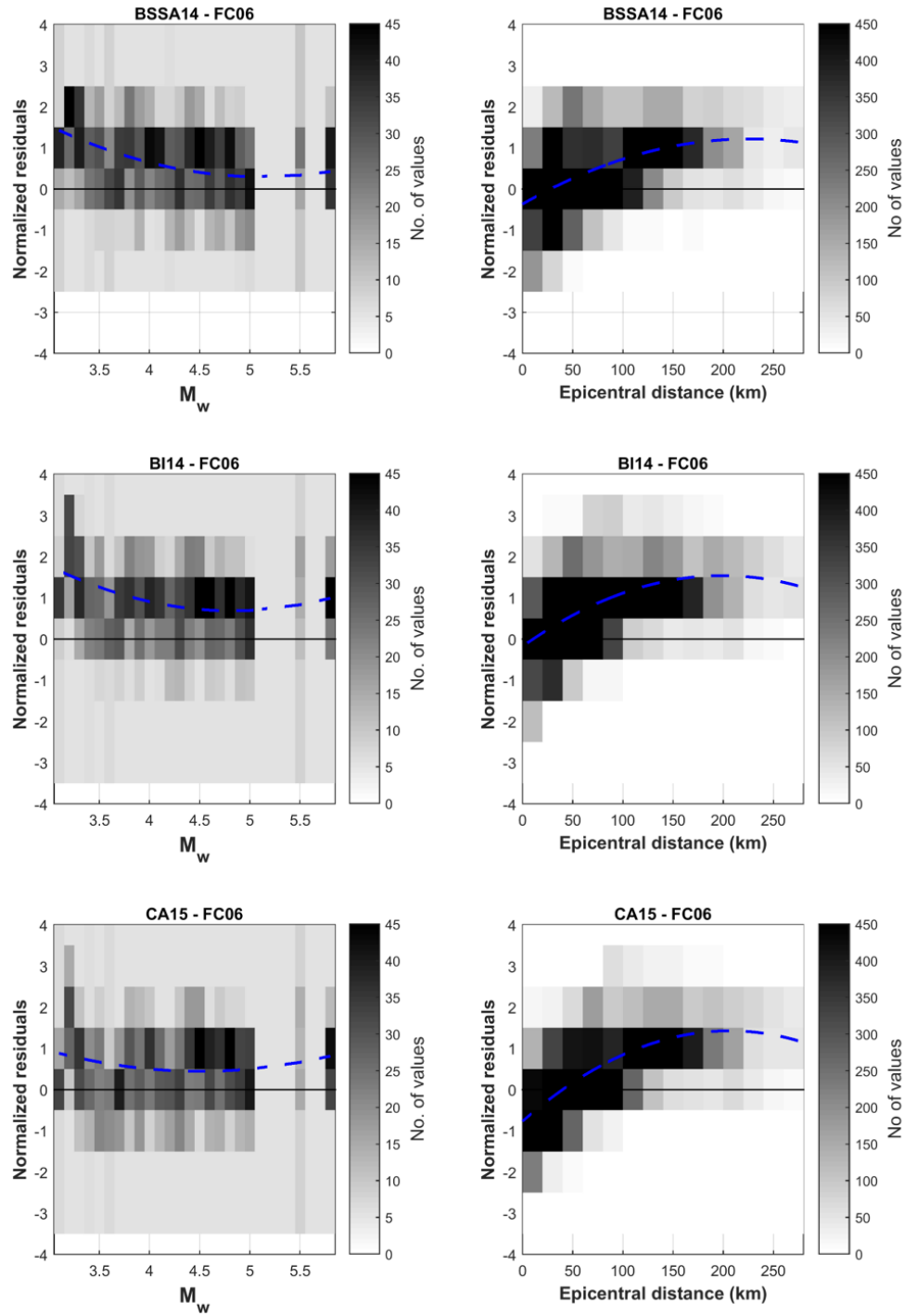


943

944 Figure 15. Comparison of six correlations from literature between PGA and intensity (grey lines: solid

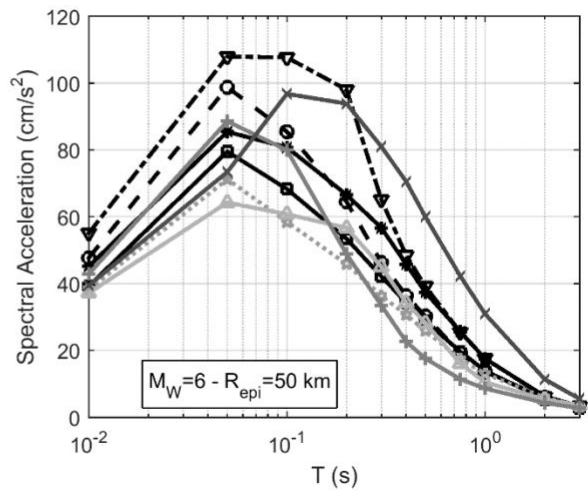
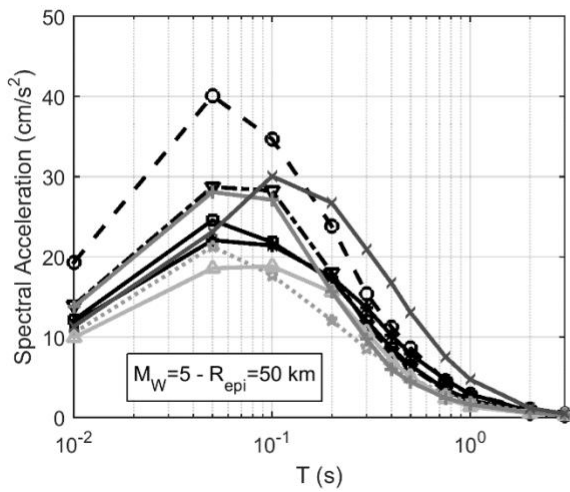
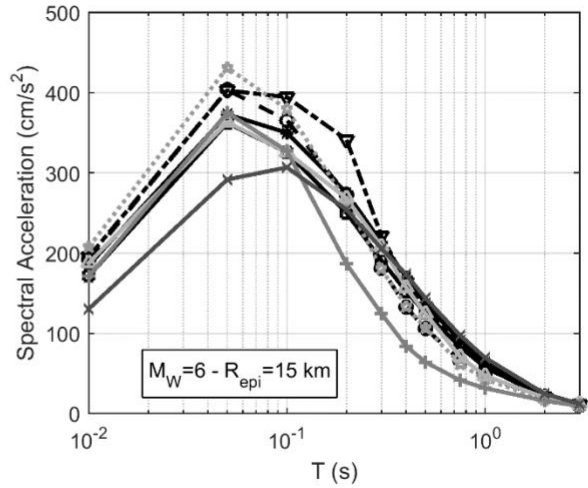
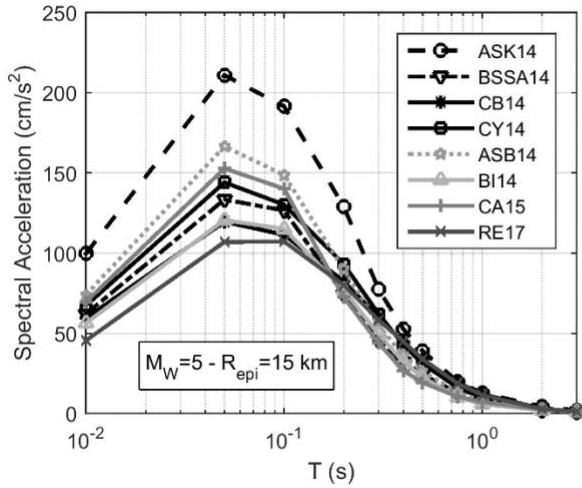
945 median prediction, dashed 5th-95th percentiles) against a subset of the UK data for which both intensities

946 and PGA were available (dots)



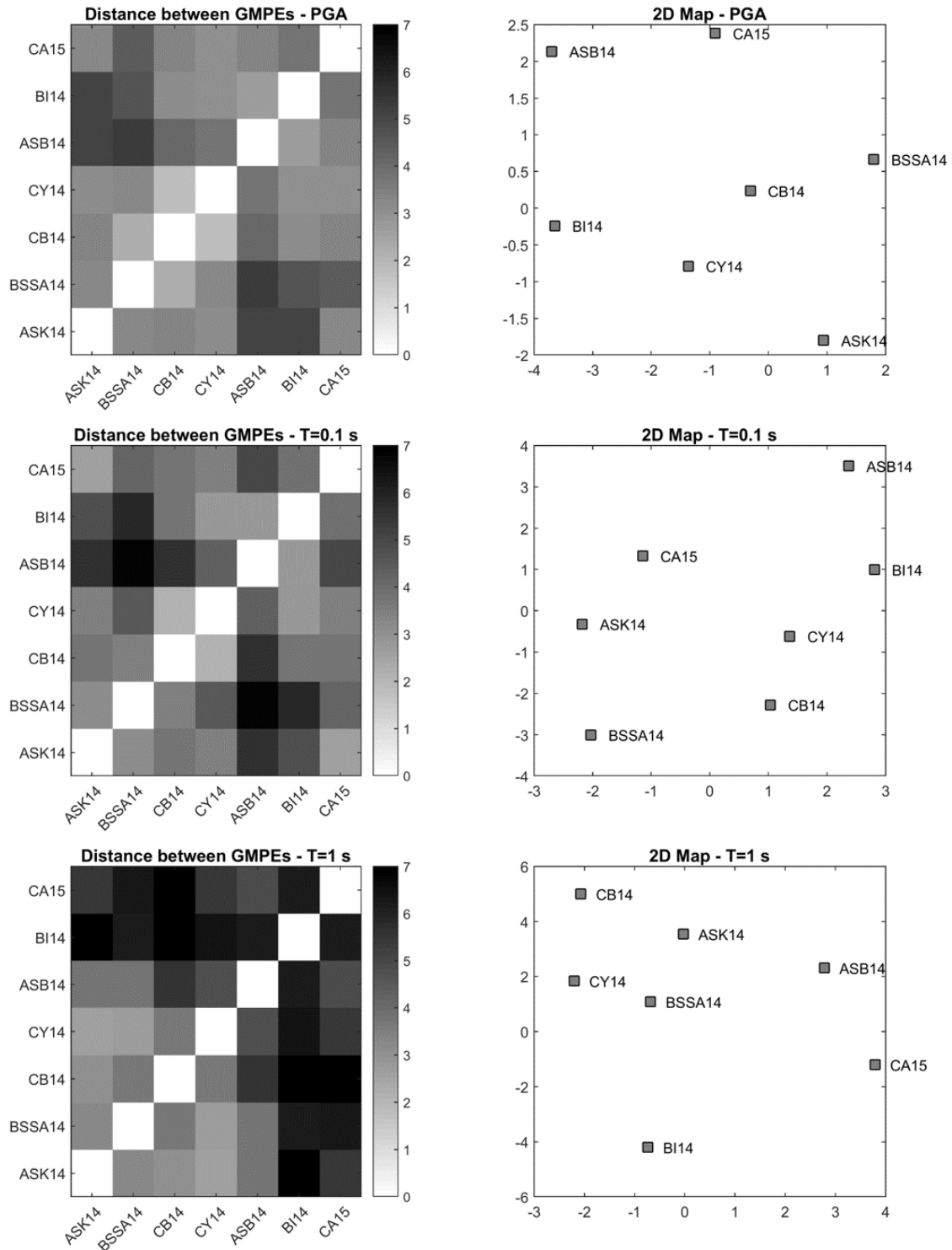
947

948 Figure 16. Examples of normalized model residuals between UK macroseismic data and
 949 predictions from three GMPEs using the GMICE from Faccioli and Cauzzi (2006), FC06.



950

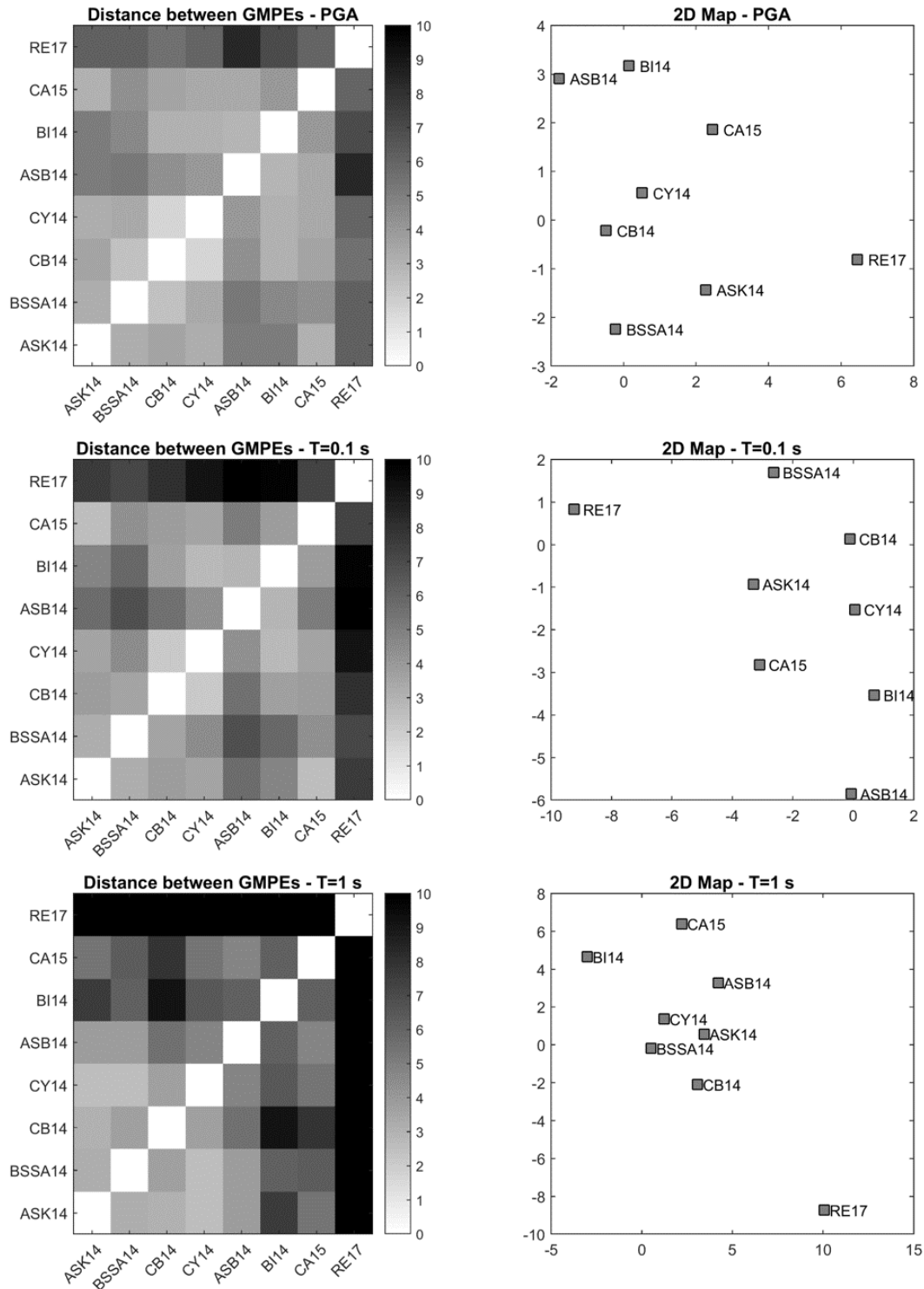
951 Figure 17. Comparisons among the response spectra predicted by the eight GMPEs at two
 952 magnitude values ($M_w=5$ and 6) and two epicentral distances ($R_{epi}=15$ and 50 km).



953

954 Figure 18. Similarities between GMPEs in terms of Euclidean distance (left) and Sammon's map

955 (right) for rock sites.



956

957 Figure 19. Similarities between GMPEs in terms of Euclidean distance (left) and Sammon's map

958 (right) for hard rock sites